Dynamic changes of depolarizing GABA in a computational model of epileptogenic brain: Insight for Dravet syndrome.

Polina Kurbatova, Fabrice Wendling, Anna Kaminska, Anna Rosati, Rima Nabbout, Renzo Guerrini, Olivier Dulac, Gérard Pons, Catherine Cornu, Patrice Nony, et al.

▶ **To cite this version:**

Polina Kurbatova, Fabrice Wendling, Anna Kaminska, Anna Rosati, Rima Nabbout, et al.. Dynamic changes of depolarizing GABA in a computational model of epileptogenic brain: Insight for Dravet syndrome.. Experimental Neurology, 2016, 283 (Pt A), pp.57-72. 10.1016/j.expneurol.2016.05.037 . inserm-01341764

HAL Id: inserm-01341764

https://www.hal.inserm.fr/inserm-01341764

Submitted on 4 Jul 2016

HAL is a multi-disciplinary open access archive for the deposit and dissemination of scientific research documents, whether they are published or not. The documents may come from teaching and research institutions in France or abroad, or from public or private research centers.

L'archive ouverte pluridisciplinaire **HAL**, est destinée au dépôt et à la diffusion de documents scientifiques de niveau recherche, publiés ou non, émanant des établissements d'enseignement et de recherche français ou étrangers, des laboratoires publics ou privés.

ACCEPTED MANUSCRIPT

Dynamic Changes of Depolarizing GABA in a Computational Model of Epileptogenic Brain: Insight for Dravet Syndrome.

P.Kurbatova[5], F.Wendling[2], A.Kaminska[1], A. Rosati[6], R.Nabbout[1], R.Guerrini[6,7], O.Dulac[1], G.Pons[1], C.Cornu[3,4,5], P.Nony[4,5], the CRESIM/EpiCRESIM study Group^, C.Chiron[1], and P.Benquet[2#].

[1] UMR 1129, Inserm- Paris Descartes University-CEA, Paris, France

[2] UMR 1099, Inserm-University Rennes1, LTSI, Rennes, France

[3] Hôpital Louis Pradel, Centre d'Investigation Clinique, INSERM CIC201/UMR5558, Bron, France

[4] CHU Lyon, Service de Pharmacologie Clinique, Lyon, France

[5]University Lyon 1, UMR 5558, CRNS, Lyon, France

[6] Pediatric Neurology Unit and Laboratories, Children's Hospital A. Meyer-University of Florence, Firenze, Italy

[7] IRCCS Fondazione Stella Maris, Pisa, Italy

[#]corresponding author

^Membership of the CRESIM/EpiCRESIM study Group is provided in the Acknowledgments.

Keywords: excitatory GABA, epilepsy, Dravet, fast-onset, seizure, depolarizing GABA, interneuron, glutamate, SCN1A, EEG, stiripentol, shunting inhibition

Highlights

- Excitatory GABA effect was implemented in a computational neural mass model
- Dynamic emergence of depolarizing GABA triggers interictal to ictal transitions
- Results suggest a major role of GABAergic interneurons in seizure onset
- Model reproduces clinical patterns found in a severe infantile epilepsy

ACCEPTED MANUSCRIPT

Abstract

Abnormal reemergence of depolarizing $GABA_A$ current during postnatal brain maturation may play a major role in paediatric epilepsies, Dravet syndrome (DS) being among the most severe. To study the impact of depolarizing GABA onto distinct patterns of EEG activity, we extended a neural mass model as follows: one sub-population of pyramidal cells was added as well as two sub-populations of interacting interneurons, perisomatic-projecting interneurons (basket-like) with fast synaptic kinetics $GABA_A$ (fast, I1) and dendritic-projecting interneurons with slow synaptic kinetics $GABA_A$ (slow, I2). Basket-like cells were interconnected to reproduce mutual inhibition mechanisms (I1->I1).

The firing rate of interneurons was adapted to mimic the genetic alteration of voltage gated sodium channels found in DS patients, *SCN1A*+/-. We implemented the "dynamic depolarizing $GABA_A$" mediated post-synaptic potential in the model, as some studies reported that the chloride reversal potential can switch from negative to more positive value depending on interneuron activity. The "shunting inhibition" promoted by $GABA_A$ receptor activation was also implemented.

We found that increasing the proportion of depolarizing $GABA_A$ mediated IPSP (I1->I1 and I1->P) only (i.e.,other parameters left unchanged) was sufficient to sequentially switch the EEG activity from background to (1) interictal isolated polymorphic epileptic spikes, (2) fast onset activity, (3) seizure like activity and (4) seizure termination. The interictal and ictal EEG patterns observed in 4 DS patients were reproduced by the model via tuning the amount of depolarizing $GABA_A$ postsynaptic potential. Finally, we implemented the modes of action of benzodiazepines and stiripentol, two drugs recommended in DS. Both drugs blocked seizure-like activity, partially and dose-dependently when applied separately, completely and with a synergic effect when combined, as has been observed in DS patients.

This computational modeling study constitutes an innovative approach to better define the role of depolarizing GABA in infantile onset epilepsy and opens the way for new therapeutic hypotheses, especially in Dravet syndrome.

Introduction

In adult brain, the excitatory/inhibitory (E/I) ratio is crucial for cortical functions. Despite increased cortical activity, individual cortical glutamatergic neurons show a stable E/I ratio because inhibitory interneurons are proportionally recruited as excitatory neurons (Xue et al., 2014). Considering its central role in the brain, the dysregulation of GABAergic interneuron function may thus lead to many pathological states, including fragile X syndrome (Olmos-Serrano et al., 2010), autism spectrum disorders (Han et al., 2012), Down syndrome (Pérez-Cremades et al., 2010), mood disorders (Lin and Sibille, 2013), chronic pain (Zeilhofer et al., 2012) and epilepsy (Fritschy, 2008), as shown in respective animal models.

The reversal potential of $GABA_A$ current shifts from a depolarized toward a hyperpolarized value during brain maturation (for recent review see (Ben-Ari et al., 2012). The embryonic excitatory effect of GABA is a key player in brain development and maturation as it triggers calcium signals, modulates DNA synthesis, proliferation, migration, differentiation of neurons and synaptogenesis (Owens and Kriegstein, 2002) (Ben-Ari et al., 2007) (Rakhade and Jensen, 2009). Depolarizing $GABA_A$ ($dGABA_A$)

ACCEPTED MANUSCRIPT

effects are no longer operating in the normal mature brain (Glickfeld et al., 2009) but have been detected in many neurological disorders(Ben-Ari et al., 2012) including epilepsy (Huberfeld et al., 2007) (Pathak et al., 2007). This constitutive $dGABA_A$ current in adult tissue is due to an abnormal downregulation of chloride transporter (Huberfeld et al., 2007; Palma et al., 2006). Moreover, a shift of $GABA_A$ reversal potential can occur dynamically within minutes when the firing rate of interneuron greatly increases. Indeed, during enhanced cortical excitation or epileptic activity, enhanced GABA release overloads the postsynaptic cell in chloride and therefore dynamically shifts the effect of GABA from hyperpolarizing to depolarizing (Alfonsa et al., 2015; Kaila et al., 1997; Lamsa and Taira, 2003).

In early life onset epilepsies, the disruption of inhibitory activity or abnormal maturation of the inhibitory system might increase global network activity and therefore evoke the re-appearance of $dGABA_A$ in postnatal tissue. During human brain development, loss-of-function of the potassium-chloride co-transporter KCC2 has been suspected to induce a failure of GABAergic inhibition, the reemergence of a depolarizing effect of GABA and consequently the trigger of early-onset severe infant epilepsy. For instance, a mutation of SLC12A5, producing a loss of KCC2 activity which impairs chloride extrusion is responsible for early-onset epileptic encephalopathy with migrating focal seizures (Stödberg et al., 2015). KCC2 missense variant KCC2-R952H was identified in an Australian family with childhood onset febrile seizures occurring between 12 months and 2.5 years of age (Puskarjov et al., 2014). Other mutations, such as R1049C, a functional variants coding for human KCC2, might be associated with idiopathic generalized epilepsy (Kahle et al., 2014).

Dravet syndrome (DS) is a relatively rare but severe infantile onset epilepsy syndrome (incidence <1/40,000) characterized by hemi- and generalized, febrile and afebrile (tonic-)clonic seizures appearing from the first year of life in an otherwise normal child. Within the second year, other seizure types may occur as well (myoclonus, atypical absences, partial seizures) and developmental delay becomes apparent, then followed by definite cognitive impairment and behavioral disorders (Scheffer, 2012). Although frequently prolonged and highly pharmacoresistant, these seizures have proven to be partially responsive to an anticonvulsive co-medication including stiripentol and the benzodiazepine clobazam (Chiron et al., 2000). *SCN1A* gene mutations (which encode the NaV1.1 α1 subunit of voltage-gated sodium channel) have been identified in about 85% children with DS (Claes et al., 2001; Marini et al., 2011).

Cellular mechanisms are unclear. On one side, a mouse model of DS due to *SCN1A* heterozygote mutation has shown a selective failure of excitability of GABAergic interneurons perturbing the E/I ratio, focusing on dissociated hippocampal neurons(Yu et al., 2006). On the other side, recent data using DS patient-derived induced pluripotent stem cells (iPSC) disclosed an unexpected increased excitability of both GABAergic and glutamatergic isolated neurons (Chopra and Isom, 2014; Jiao et al., 2013; Liu et al., 2013). Computational modeling has the potential to test such views.

In this study, we started from the hypothesis that in this infantile epilepsy, constitutive (developmental) and dynamic GABAergic signaling is severely impaired. We developed a physiology-based computational model in order to investigate some possible pathophysiological causes of DS and to test the mechanism of action of some drugs recommended for this condition. We used a lumped-parameter approach (often referred to as “neural mass”) lying at the level of cortical neuronal population to compare simulated EEG activity with real EEG activity recorded in patients with DS.

ACCEPTED MANUSCRIPT

Methods

The "physiological" neural mass model

Neural mass models have been commonly used to study epileptic-like activity in EEG signals. We started from the model described in (Huneau et al., 2013; Molaee-Ardekani et al., 2010; Wendling et al., 2012, 2002) see (Wendling et al., 2015) for recent review. In order to simulate epileptic signals generated in the cerebral cortex, we started from a physiologically plausible computational model at the level of neuronal assembly. For detailed description of the model, readers might refer to (Molaee-Ardekani et al., 2010).

The model is composed by the following sub-populations: (i) pyramidal cells (P), receiving excitatory feedback from other pyramidal cells and inhibitory feedback signals from (ii) soma- and proximal dendrite-targeting cells (I1: basket-like cells and chandelier-like cells mediating $GABA_A$, fast currents), and (iii) dendrite-targeting cells (I2: neurogliaform-like cells mediating $GABA_A$, slow currents) (see Fig 1A). Unlike detailed network models, neural mass models do not explicitly represent individual cells and their architecture (i.e., dendrites, soma or axons) but are mainly based on synaptic connections of distinct populations of neurons. Somatic-targeting interneurons I1 refers to cells that generate PSP with a physiologically relevant time constant, similar to the IPSP produced by basket cells or chandelier cells (Molaee-Ardekani et al., 2010). Although macroscopic, this model relies on neurophysiological data and has two essential features. First, their parameters relate to excitatory and inhibitory processes taking place in the considered neuronal tissue. Second, the temporal dynamics of their output (analogous to a local field activity) can be directly compared to those reflected in real signals recorded with electrodes placed in the cerebral cortex. Indeed, it can be assumed that field potentials reflect overall dynamics arising from interconnected populations of principal neurons and interneurons.

According to the neural mass modeling approach, each subpopulation was characterized by two functions. First, the 'pulse-to-wave' function was a 2nd order linear transfer function $h(t) = Wwte^{-wt}$ that transformed the average presynaptic pulse density of action potentials coming to the subpopulation of neurons into an average postsynaptic membrane potential which can be excitatory, slow inhibitory or fast inhibitory.

As depicted in Figure 1A, the model implements three types of 'pulse-to-wave' functions. The first one is AMPAergic and describes the synaptic transmission among pyramidal cells (P to P) as well as the excitatory input to both subpopulations of interneurons (P to I1 and P to I2). Its impulse response corresponds to an average EPSP and is given by the equation:

$$h_{AMPA}(t) = \frac{W_{AMPA}}{\tau_{AMPA}} t.e^{-t/\tau_{AMPA}} \quad \text{(eq. 1).}$$

The second one is GABAergic and describes the inhibitory input (at the level of GABAa,slow receptors) from interneurons I2 to pyramidal cells (I2 to P) and to interneurons I1 (I2 to I1). Its impulse response is given by the equation:

$$h_{GABAa,s}(t) = \frac{W_{GABAa,s}}{\tau_{GABAa,s}} t\, e^{-t/\tau_{GABAa,s}} \quad \text{(eq. 2).}$$

ACCEPTED MANUSCRIPT

Finally, the third one is also GABAergic and describes the inhibitory input (at the level of GABAa,fast receptors) from interneurons I1 to pyramidal cells (I1 to P) and among interneurons I1 (I1 to I1, mutual inhibition). In this case,

$$h_{GABAa,f}(t) = \frac{W_{GABAa,f}}{\tau_{GABAa,f}} t\, e^{-t/\tau_{GABAa,f}} \qquad \text{(eq. 3)}$$

In the function $h(t) = Wwte^{-wt}$, $W$and w respectively determine the amplitude and time constant of the average receptor-mediated postsynaptic potentials. Depending on the type of the considered interacting sub-populations,$W = W_{AMPA}$, $W = W_{GABAa,s}$ or $W = W_{GABAa,f}$ and $w = 1/\tau_{AMPA}$, $w = 1/\tau_{GABAa,s}$ or $w = 1/\tau_{GABAa,f}$.

It is worth noting that the time constant used in a given $h(t)$function determines both the rise time (t_{rise}= 1/w) and the decay time (t_{decay} = 3.146/w) of the PSPs that are designated to match those of actual PSPs.

Second, the 'wave-to-pulse' function transforms the average postsynaptic membrane potential of a subpopulation of neurons into an average pulse density of action potentials fired by the neurons. For each given subpopulation X, the 'wave-to-pulse' function was modeled by a nonlinear function of sigmoid shape $S_{\mathrm{x}}(\vartheta) = Q_{\mathrm{x}}^{\max}/(1 + e^{\mathrm{r_x}(\theta_{\mathrm{x}} - \vartheta)})$ which accounts for saturation and threshold effects taking place at the soma. Here, $Q_{\mathrm{x}}^{\max}$determines the maximum firing rate of the neuronal population, θ_{x} the PSP for which a 50% firing rate is achieved, and $\mathrm{r_x}$the steepness of the sigmoidal transformation.

In order to derive the ordinary differential equations that govern the model, one must notice that each one of the 7 'pulse-to-wave' functions (P to P, P to I1, P to I2, …, I1 to I1) introduces a second order linear transfer function $h(t) = Wwte^{-wt}$and a corresponding second order ordinary differential equation (ODE):

$$\ddot{z}(\mathrm{t}) = Wwx(t) - 2w\dot{z}(t) - w^2 z(t) \qquad \text{(eq. 4)}$$

where *x(t)* and $z(t)$ are respectively the input (firing rate) and output signals (PSPs) of each linear transfer function$h(t)$. From equations 1 to 4, the following set of differential equations was established:

ACCEPTED MANUSCRIPT

$$\begin{cases} \ddot{z}_0(t) = \frac{W_{AMPA}}{\tau_{AMPA}} S_p\left(\vartheta_p(t)\right) - \frac{2}{\tau_{AMPA}}\dot{z}_0(t) - \frac{1}{\tau_{AMPA}^2} z_0 \text{(P to P)} \\ \ddot{z}_1(t) = \frac{W_{AMPA}}{\tau_{AMPA}} S_{I1}\left(\vartheta_P(t)\right) - \frac{2}{\tau_{AMPA}}\dot{z}_1(t) - \frac{1}{\tau_{AMPA}^2} z_1 \text{(P to I1)} \\ \ddot{z}_2(t) = \frac{W_{GABAa,f}}{\tau_{GABAa,f}} S_{I1}\left(\vartheta_{I1}(t)\right) - \frac{2}{\tau_{GABAa,f}}\dot{z}_2(t) - \frac{1}{\tau_{GABAa,f}^2} z_2 \text{(I1 to I1)} \\ \ddot{z}_3(t) = \frac{W_{GABAa,f}}{\tau_{GABAa,f}} S_P\left(\vartheta_{I1}(t)\right) - \frac{2}{\tau_{GABAa,f}}\dot{z}_3(t) - \frac{1}{\tau_{GABAa,f}^2} z_3 \text{(I1 to P)} \\ \ddot{z}_4(t) = \frac{W_{AMPA}}{\tau_{AMPA}} S_{I2}\left(\vartheta_P(t)\right) - \frac{2}{\tau_{AMPA}}\dot{z}_1(t) - \frac{1}{\tau_{AMPA}^2} z_1 \text{(P to I2)} \\ \ddot{z}_5(t) = \frac{W_{GABAa,s}}{\tau_{GABAa,s}} S_P\left(\vartheta_{I2}(t)\right) - \frac{2}{\tau_{GABAa,s}}\dot{z}_5(t) - \frac{1}{\tau_{GABAa,s}^2} z_5 \text{ (I2 to P)} \\ \ddot{z}_6(t) = \frac{W_{GABAa,s}}{\tau_{GABAa,s}} S_{I1}\left(\vartheta_{I2}(t)\right) - \frac{2}{\tau_{GABAa,s}}\dot{z}_6(t) - \frac{1}{\tau_{GABAa,s}^2} z_6 \text{(I2 to I1)} \end{cases}$$

where $z(t)$ is the state vector of the system and where $\vartheta_x$is the average membrane potential in each subpopulation X (P, I1 or I2), described as follows:

$$\vartheta_P(t) = C_{PP} z_0(t) - C_{I1P}(z_3(t) - \underbrace{\alpha_{I1P} S_{I1}^{t^-}}_{\text{GABAdepolarization I1->P}} + \underbrace{\beta_{I1P} S_{I1}^{t^-} \cdot \tau_{GABAa,f}}_{\text{Shunting inhibition}}) - C_{I2P}(z_5(t) - \underbrace{\alpha_{I2P} S_{I2}^{t^-}}_{\text{GABAdepolarization I2->P}} +$$

$$+ \underbrace{\beta_{I2P} S_{I2}^{t^-} \cdot \tau_{GABAa,s}}_{\text{Shunting inhibition}}) + q(t) + p(t), \qquad \text{(eq. 5)}$$

$$\vartheta_{I1}(t) = C_{PI1} z_1(t) - C_{I1I1}(z_2(t) - \underbrace{\alpha_{I1I1} S_{I1}^{t^-}}_{\text{GABAdepolarization I1->I1}} + \underbrace{\beta_{I1I1} S_{I1}^{t^-} \cdot \tau_{GABAa,f}}_{\text{Shunting inhibition}}) - C_{I2I1}(z_6(t) -$$

$$- \underbrace{\alpha_{I2I1} S_{I2}^{t^-}}_{\text{GABAdepolarization I2->I1}} +$$

$$+ \underbrace{\beta_{I2I1} S_{I2}^{t^-} \cdot \tau_{GABAa,s}}_{\text{Shunting inhibition}}) + q(t), \qquad \text{(eq.6)}$$

$$\vartheta_{I2}(t) = C_{PI2} z_4(t) + q(t).$$

Parameters C_{XX}, are referred to as connectivity constants between subpopulation X and subpopulation X'. Physiologically, C_{XX}, is interpreted as an average number of synaptic contacts. Formally, these parameters act as gains in the feedback loops interconnecting the three subpopulations.

The influence from neighboring or distant populations was modeled by an excitatory input $p(t) = \bar{p} + N(0, \sigma)$, represented by a Gaussian noise. In addition, a very slow oscillation mimicking delta waves often encountered in DS was added to each subpopulation average membrane potential to increase the

ACCEPTED MANUSCRIPT

realism of simulated EEGs. This slow oscillation is given by $q(t) = A.\sin(2\pi f t)$, with $A = 0.05$ and $f = 0.33$ Hz.

In the above equations, $S_{\mathrm{x}}^{t^-} = S_{\mathrm{x}}\left(\vartheta_{\mathrm{x}}(t^-)\right)$ denotes the average firing rate of subpopulation X at the previous integration step t^-. This average firing rate value is involved in the two mechanisms implemented in the model, namely the GABA depolarization and the shunting inhibition effects described below.

The simulated LFP is computed as the summation of PSPs (either excitatory or inhibitory) at the level of pyramidal cells. It is well admitted that these pyramidal cell PSPs is the main contribution to LFP (Niedermeyer and Lopes da Silva, 2005). According to the neural mass modeling approach, the influence from neighboring or more distant populations onto the considered population is modeled by an excitatory input, itself represented by a Gaussian noise of variance σ^2. Note that when the system operates on a fixed point and when σ is low, the output of the firing rate function (sigmoid function S_X) appears as almost constant, as depicted in Fig 2 B,C,D. Finally, model parameters are documented in Table 1 along with values used in the simulations reported in Figs 2 to 6.

From physiological to pathological brain activity

The above described model incorporates some (patho)physiological mechanisms that are likely to play a key role in the generation of epileptic activity in the infantile onset epilepsy Dravet syndrome. These mechanisms are described hereafter.

Depolarizing GABA.

GABA-elicited currents cause hyperpolarizing or depolarizing postsynaptic potentials depending on the $GABA_A$ reversal potential (E_{GABA}). Hyperpolarizing GABA was previously considered in mean-field models (Goodfellow et al., 2011; Wendling et al., 2002). Acute intracellular chloride $[Cl^-]_i$ accumulation results in a shift of the E_{GABA} in the depolarizing direction toward resting membrane potential (V_{rest}). As a consequence, E_{GABA} may rise above V_{rest}, thus leading to GABAergic induced depolarizations (Figs. 1C and 1D).

Activity-dependent $[Cl^-]_i$ changes were studied in a computational model of hippocampal cells, but not in the context of epilepsy (Jedlicka et al., 2011). The authors showed that in case of intense GABAergic background activity (during high frequency firing of interneurons), E_{GABA} changed in both somatic and dendritic compartments. Therefore, in our model, the depolarizing effect was implemented for both types of synapses ($GABA_A$, slow and $GABA_A$, fast).

In the neural mass model there is no access to individual cellular membrane potentials but to average membrane potentials of a subpopulation of neurons. Although direct account for E_{GABA} is not straightforward in this modeling approach, average PSPs are explicitly represented at each subpopulation and can therefore be modified to account for excitatory GABAergic potentials, as illustrated in Figure 1D.

ACCEPTED MANUSCRIPT

For depolarizing GABA:
$-C_{XX'}.(-\alpha_{XX'}.S_X^{t^-})$ > 0 (as $\alpha_{XX'} > 0$).

For hyperpolarizing GABA:
$-C_{XX'}.z_k(t) < 0$

where X' denote the target subpopulation of neurons receiving PSPs from the source subpopulation X and where Zk denote the PSP exchanged at the interface of subpopulations X and X'.As this quantity is positive, an increase of the mean membrane potential is achieved (depolarizing effect) and weighted by the firing rate of subpopulation X.

This mathematical expression allows for the presence of excitatory GABAergic PSPs referred to as "static" GABAergic depolarization that is likely to occur in epileptic tissue when some chloride transporters are not sufficiently expressed in a subpopulation of neurons (Huberfeld et al., 2007; Palma et al., 2006). It is assumed that changes in E_{GABA} are spatially non-uniform across the population. It is likely that within a subpopulation of pyramidal cells some neurons get hyperpolarized by GABA (expressing a large amount of chloride transporters) and some others get depolarized by GABA (expressing a few chloride transporters). For example, in human mTLE, $GABA_A$-mediated IPSPs reversed at depolarizing potentials in 20% of pyramidal cells (Huberfeld et al., 2007).

In addition, $\alpha_{XX'}$ can be made time-dependent to represent a "dynamic" GABA depolarization effect. This can be easily achieved by adding extra ODEs to the model in the form of $\frac{d\alpha_{XX'}}{dt} = K$ where *K* is used to adjust the rate of change of $\alpha_{XX'}$ with time (linear function). When *K > 0,* an amplification of the $GABA_A$ depolarizing effect occurs in the model. Indeed, the increase of the mean membrane potential of subpopulation P leads to an increase of its firing rate and thus to an increase of the excitatory drive onto interneurons I1 and I2 and ultimately of their respective firing $S_{I1}^{t^-}$ and $S_{I2}^{t^-}$ (Fig 1E).

Shunting inhibition. The other effect on the postsynaptic membrane mediated by GABAergic events is called 'shunting inhibition'. That is a form of postsynaptic potential inhibition owing to an increase of the postsynaptic membrane conductance due to the sustained activation of $GABA_A$ receptors and the opening of ion channels.

This shunting inhibitory effect always remains, independently of the effect of GABA (depol- or hyper-polarizing). The shunting inhibition cannot be directly coded in the mesoscopic model because the membrane resistance of the cells is not explicitly implemented. Therefore we mathematically represented this effect by modifying the membrane potential in pyramidal cells, fast and slow interneurons depending on the firing rate of interneurons and weighted by the IPSP time constant. As depicted in equations5 and 6, the mathematical expression for representing shunting inhibition was $-C_{XX'}.\beta_{XX'}.S_X^{t^-}.\tau_{GABAa}$. As this quantity is negative, an inhibitory effect is achieved in the model, and it increased when the firing rate of interneurons increases.

SCN1A mutation. We adjusted variables to account for the mutation of the gene *SCN1A* encoding for the NaV1.1 α-1 subunit of the voltage-gated sodium channel (VGSC) related to Dravet syndrome (Claes et al., 2001; Escayg et al., 2000; Harkin et al., 2007; Scheffer and Berkovic, 1997). All patients selected for the present study were carrying a *SCN1A* mutation (see Table 2). Mutant *SCN1A*$^{+/-}$ mouse models of

ACCEPTED MANUSCRIPT

DS robustly identified an alteration of the expression of VGSC specifically in GABAergic interneurons as a cause of selective loss of sodium current affecting their firing properties which results in epilepsy (Yu et al., 2006). In order to mimic such an alteration we adapted the sigmoid functions describing the average firing rate as a function of the average PSP at the level of fast and slow interneurons in our macroscopic model (see Fig 1B). The sigmoid functions of the firing rate of both perisomatic- I1 and dendritic- I2 projecting interneurons were intentionally modified compared to pyramidal cells (Table 1).

Virtual pharmacology

We studied the pharmacological impact on neuronal populations of two antiepileptic drugs (AED), stiripentol and clobazam, that we selected for their clinical relevance in Dravet syndrome (DS) and their known mechanism of action on $GABA_A$ receptors. Enhanced activity of $GABA_A$ receptors increases the shunting effect and may therefore inhibit seizures. Stiripentol is the only AED currently approved in DS, having proven to reduce seizure frequency significantly more than placebo, when associated to clobazam and valproate within two independent randomized controlled trials performed in children with DS (Chiron et al., 2000; Kassaï et al., 2008). Stiripentol directly acts on the $GABA_A$ receptors by enhancing the opening duration of the chloride channel in a dose-dependent manner (Quilichini et al., 2006). In order to reproduce this effect, we prolonged IPSC decay time (t_{decay}) in the model by increasing the decay-time constant ($1/b$) and ($1/g$) of IPSPs to 125% for 30 µM, 200% for 100 µM and 235% for 300 µM of STP. By contrast benzodiazepines have a major effect on $GABA_A$ mediated IPSC amplitude (Hájos et al., 2000). To introduce benzodiazepine action in the model we increased parameter W_{GABA}, representing the amplitude of IPSC (125% for 1 µM, 178% for 10 µM and 200% for 100 µM). The drug concentrations of stiripentol and benzodiazepine used in the model were selected based on their therapeutical relevance(Quilichini et al., 2006, 2003).

Neuronal activity and clinical data

In the present study we used scalp EEG signals recorded in patients with DS as a reflection of real neural activity to be compared with LFPs simulated by our computational model. We compared qualitatively the temporal dynamics of both simulated and real signals, i.e. the time constant and the shape of the interictal and ictal patterns. It is worth noting that the essential signal features being compared are related to the morphology and spectral content. In our case, the amplitude is meaningless since we didn't solve the forward EEG problem (i.e., from cortical sources to signals collected at scalp electrodes).

Dravet patients (n=4) were selected for the present study from the two reference centers for infantile onset epilepsy involved in the CRESIM project in France and Italy. Selection criteria were the following: over 2 years of age, complete clinical features of Dravet syndrome, *SCN1A* mutation, at least one digitalized prolonged video-EEG recording available, at least one convulsive seizure with (tonic-)clonic component recorded. Four patients were selected; individual data are shown in Table 2.

Results

The computational model of neocortical neuronal populations (Molaee-Ardekani et al., 2010), (Fig 1A) was modified to include : 1) the reduced firing rate of interneurons (due to $SCN1A^{+/-}$ mutation) (Fig 1B);

ACCEPTED MANUSCRIPT

2) a sinusoidal fluctuation to mimic delta 1 wave and 3) a proportion of $dGABA_A$ (Figs.1C, D) (see Methods). To mimic activity-dependent chloride accumulation into the cells (Fig 1E), we increased the proportion of $dGABA_A$ in I1->P, I1->I1 and I2 ->P as a function of interneuronal firing rate.

Simulated neural activity

Interictal to ictal transition. Dynamic depolarizing $GABA_A$ from I1->P and I1->I1 was simulated (Fig. 2). Parameters α_{I1I1} and α_{I1P} are time-dependent and were varied progressively (from 0 to 0,007 and 0,017 respectively) during 50 seconds. Continuous change of these two parameters leads to transition from interictal to seizure-like activity, FO activity, seizure termination, as well as to the sharp increase in I1 and I2 firing rates.

The model was configured with parameters mimicking a highly excitable network (increased P->P excitation of cortical cells, decreased inhibition I1->P, and constitutive-static- $dGABA_A$), but when the amount of $dGABA_A$ did not vary, the LFP stayed below the threshold of seizure generation (Fig 2A, first 22 seconds of the trace). When the proportion of $dGABA_A$ at the somatic-projecting Interneurons I1 (to I1 and Pyr) increased (I1) the model produced a mean-field activity that sequentially and spontaneously switched from background activity to successively 1) isolated interictal spikes, 2) fast onset activity, 3) ictal like activity and finally 4)seizure-like activity termination (Fig 2A).

A slow variation of the amount of depolarizing GABA is necessary to capture the time course of the alternating sequence of seizure-like event. Slow variation of this parameter evokes the sequential generation of interictal to ictal events and also produced a slow drift of the offset.

The identified interictal/ictal transition pattern is quite robust to variations of model parameters alpha_I1_P and alpha_I1_I1. Up to 40% change of both parameters, the sequence of phases (background activity, sporadic/rhythmic spikes, fast onset activity, ictal activity) is preserved although some variations are observed, typically in the duration of each phase (S1 Fig).

Fast Onset activity. Interestingly, the model produced high frequency oscillations at the onset of the seizure-like activity. The intrinsic frequency of the preictal fast onset activity decreased from 105 to 90 Hz. As shown on the time-frequency spectrum analysis, this chirp-like activity (Fig 2B, bottom) was reminiscent of the patterns showing fast frequency changes often encountered in partial epilepsies (Schiff et al., 2000) (Cosandier-Rimélé et al., 2012). The average firing rate of the three subpopulations of neurons (P, I1 and I2) is depicted in Fig 2C. The activity in the subnetworks differed during the dynamical interictal to ictal transition that occurs in the LFP simulated by the model. During the fast onset oscillations, pyramidal cells remained almost silent (at least the firing rate is low). Conversely, the firing rate of basket cells greatly increased and induced the fast onset activity visible in the LFP (Fig 2C), as exemplified in the inset. The model predicted that GABAergic postsynaptic potential switch from inhibitory to excitatory occurred as a consequence of the strong mutual connections of basket cells (I1→I1 = 15 and activity-dependent dGABA I1→I1 = 0.07). Depolarizing GABA, within these mutual interconnections, induced an oscillatory GABAergic activity between interneurons leading to this fast onset activity (Fig 2B). Indeed, reducing mutual inhibition I1→I1 suppressed fast onset activity (Fig 2D).

Seizure initiation. Before seizure onset, a high frequency discharge of somatic-projecting GABAergic interneurons was generated by the model. Consequently the pyramidal cells were strongly inhibited

ACCEPTED MANUSCRIPT

and remained silent (Fig 2C). Moreover the high firing rate of GABAergic interneurons generated an increase of the activity-dependent $dGABA_A$ onto pyramidal cells and therefore a massive drop of inhibition that permitted seizure initiation.

Removing activity-dependent $dGABA_A$ from I1 onto pyramidal cells suppressed interictal event, fast onset and seizure activity (Fig 2D, right). Removing depolarizing $GABA_A$ from dendritic –projecting slow interneurons (type 2, I2) to pyramidal cells did not change the induction of interictal spikes, emergence of fast onset activity, seizure like activity and seizure termination (Fig 2D, left). However, removing depolarizing $GABA_A$ between I1 to I1 connections or I1 to pyramidal cells suppressed the fast onset activity seen at seizure initiation. In this configuration, depolarizing $GABA_A$ only on pyramidal cells (I1->P and I2->P) was not sufficient to trigger seizures (Fig 2D, middle).

When seizures started, the firing rate of pyramidal cells alternatively switched from the minimum to the maximum, in phase opposition to the activity of basket cells. Finally, when the proportion of depolarizing $GABA_A$ became too prominent in pyramidal cells and interneurons, the seizure stopped (Figs. 2A,B,C). The model also produced a pronounced slow fluctuation of the background activity reminiscent of delta-wave oscillations that emerged prior to the fast onset activity and after the seizure- like activity.

Overall the model predicted that progressive changes from inhibitory to excitatory GABAergic post-synaptic potential within the mutual inhibitory loop (I1-I1) triggered fast onset activity. These mechanisms lead to an increase of firing rate of interneurons and therefore an activity-dependent increase of $dGABA_A$ onto pyramidal cells, resulting in a collapse of inhibition that initiates seizure like activity.

Simulated compared to real neural activity

In Dravet syndrome (DS) EEG patterns are polymorphic and usually different from one patient to another, thus individual examination is crucial. We therefore compared simulated signals to real recordings for each DS patient separately.

Interictal activity. Multifocal polymorphic interictal spikes were found in patient 1 as exemplified in (Fig 3B). In the model, for a stronger excitatory input P compared to configuration 1 (mean Noise input PYR 3,6 instead of 3.2) and a ten times lower proportion of $dGABA_A$ from I1->P, the model produced series of polymorphic epileptic spikes when the proportion of the latter increased (Fig 3A). In this case the morphology was progressively switching from slow polyphasic spikes (Figs. 3A, a and b) followed by a small wave to sharper biphasic spikes (Fig 3A, c). Note that the amplitude of the negative phase increased with the proportion of $dGABA_A$.

Typical biphasic sharp spikes found in patient 2 (Fig 3B, bottom left) were reproduced by the computational model (bottom right). This common shape of epileptic spikes accompanied the peculiar interictal EEG pattern constituted by diffuse slow bi-triphasic spikes described in a subpopulation of DS patients (Nabbout et al., 2008). Strikingly, almost all kind of epileptic spike shapes (i.e., single spike, triphasic spike, biphasic spike, spike with/without following waves of small/large amplitude) could be obtained by only changing the magnitude of $dGABA_A$ at synapses between I1→P and I1→I1(Fig 3A, a,b, c).

ACCEPTED MANUSCRIPT

We observed in DS patient 2 that the shape of epileptic spikes features could evolve in a few seconds from monophasic to biphasic spikes with a small, medium or strong negative phase, following a positive phase (Fig 3C, upper). The rapid changes of spike morphology could be reproduced by the computational model by linearly increasing the proportion of $dGABA_A$ from I1->P (Fig 3C, bottom). The increases mimic the loading of intracellular chloride in pyramidal cells due to the increase of GABA release from basket cells onto principal glutamatergic neurons.

Ictal activity. We investigated model configurations that could reproduce different kinds of EEG seizure patterns. Since activity-dependent synaptic plasticity is very pronounced during brain development (Chaudhury et al., 2016), especially after experiencing seizures (Debanne et al., 2006; Lopantsev et al., 2009). Consequently, it is very likely that the strength of synaptic connections between neuronal subpopulations is specific to each patient. For these reasons distinct synaptic strengths were used for patient 1,2,3, and 4. As the features of these patterns seemed to be similar from one event to the next, at least for a few seconds, we looked for model configurations with sustained $dGABA_A$ (fixed values).

The first pattern encountered in patient 3 was a succession of sharp spikes. The model was able to reproduce this pattern when a constant high level of $dGABA_A$ was introduced in the auto inhibition loop between somatic projecting interneurons I1 (I1->I1) (Fig 4A). Strengthening this auto inhibitory loop, but also introducing a large proportion of $dGABA_A$ from somatic projecting interneuron I1->Pyramidal cells, mimicked the ictal pattern found in patient 1(Fig 4B). However, if the large proportion of $dGABA_A$ was not computed in the somatic but in the dendritic projecting interneurons (I2) to the pyramidal cells, it led to the ictal pattern of patient 4 (Fig 4C). Finally increasing $dGABA_A$ only at the synapses from I1->P led to the pattern illustrated in Fig 4D, reproducing the ictal activity of patient 2.

Over longer duration recordings, the EEG ictal pattern of DS patient 3 evolved with time (Figs. 5A and B), characterized by the emergence of a slow wave following the sharp spikes. This behavior was reliably reproduced by decreasing the amount of $dGABA_A$ between fast interneurons (I1->I1), in steps. These results suggest that, at least in some patients, the seizure onset is characterized by a proportion of $dGABA_A$ that abruptly increases within the inhibitory loop and then progressively returns to normal values.

Simulated Pharmacology

We studied the virtual pharmacological effect of $GABA_A$ receptor targeting drugs on seizures induced by the progressive contribution of $dGABA_A$(Fig 6A). In the model, benzodiazepine (BZD) induced a dose-dependent increase of $GABA_A$ current amplitude whereas stiripentol induced a dose-dependent increase of $GABA_AR$ opening time (i.e. IPSP duration) according to the literature (Quilichini et al., 2006; Rogers et al., 1994), see Methods.

Simulations indicated that both BZD (1 to 100 µM) and stiripentol (30-300µM) were able to reduce the severity of the seizure-like activity, but they did not fully prevent ictal like patterns when tested separately (Figs. 6A, B, C, D). Interestingly combining moderate concentrations of both drugs (STP100 + BZD100 or STP300+BZD10) prevented the emergence of an ictal like pattern (Figs.6A, D), suggesting a synergic effect between stiripentol and BZD.

ACCEPTED MANUSCRIPT

Discussion

Model Predictions

Our computational model of a neocortical assembly of neurons in a key infantile-onset epilepsy, Dravet syndrome, leads to several predictions. First, activity-dependent drift of E_{GABA} toward more positive value is generated within highly interconnected perisomatic projecting GABAergic interneurons forming mutual inhibition loops and evokes fast onset activity, prior to pyramidal cells activity. Second, introducing $dGABA_A$ within this inhibitory loop increases the interneuronal firing rate on pyramidal cells and, as a consequence, generates activity-dependent $dGABA_A$. The switch from IPSP to GABAergic EPSP on pyramidal cells abruptly generated a collapse of inhibition and evoked seizure-like activity. Third, without changing the strength of synaptic connections or the degree of brain network excitability (network parameters), the activity-dependent switch GABAergic IPSP to EPSP in a subpopulation of cells is able to sequentially trigger interictal epileptic spikes, fast onset activity, seizure like activity and seizure termination. Fourth**,** modulating the degree of alteration of GABAergic IPSP allowed us to reproduce the individual EEG features observed in 4 different patients with Dravet syndrome. Fifth**,** the model suggests that combination of BZD and STP is synergic to stop seizure activity in Dravet syndrome, because BZDs enhance inhibition whereas STP maximizes the shunting inhibition even if GABA produces EPSP.

Paradoxical effect of GABAergic neurons impairment

Mutations in the gene encoding *SCN1A*, are associated with a spectrum of epilepsy syndromes, including Dravet syndrome (Claes et al., 2001).This gene encodes for the NaV1.1 α1 subunit of the voltage gated sodium channel and non-sense mutation decreases the excitability of GABAergic somatostatin and PV interneurons (Cheah et al., 2012; Tai et al., 2014). This impairment of fast somatic projecting GABAergic neurons induces hyperexcitability in the network. In our model we therefore decreased the sigmoid function of the firing rate of both somatic projecting and dendritic projecting interneurons.

Paradoxically, our results suggest that the decrease of interneurons firing rate (and therefore the amount of inhibition in the networks) facilitates the dynamic switch toward depolarizing E_{GABA} for two reasons. First, it would decrease the inhibitory loop of mutual Basket-Basket inhibition. Second, the decrease of interneuron function might induce hyperexcitability of glutamatergic neurons, extrasynaptic glutamate release and extrasynaptic NMDAR overactivation and KCC2 cleavage (see discussion below). Indeed, the decrease of firing rate of interneurons would dynamically increase the excitability of the GABAergic inhibitory loop and facilitate the emergence of depolarizing GABA within the networks.

Conversely to animal studies, recent findings showed an increase of sodium current in bipolar and pyramidal neurons measured in human IPSC obtained from DS patient, leading to hyperexcitability of these cell types (Liu et al., 2013). Our computational study also predicts that interneuronal hyperexcitability induced directly by an increase of sodium current in interneurons or indirectly by an increase of pyramidal cell firing would both induce a dynamic shift toward $dGABA_A$.

Depolarizing GABA in epilepsy

ACCEPTED MANUSCRIPT

"Depolarizing $GABA_A$" has been introduced in our computational model because aberrant reappearance of E_{GABA} toward more positive values in a subpopulation of neurons and reduced GABAergic IPSP has long been proposed to underlie the pathogenesis of seizures in the immature brain (Ben-Ari et al., 2012, 2007; Holmes et al., 2002; Rakhade and Jensen, 2009) and hence the high incidence of early life epilepsies(Briggs and Galanopoulou, 2011).

Cellular mechanisms. The presence of depolarizing GABA effect might be crucial for several steps of immature brain development such as cell proliferation, neurogenesis, neuronal migration and differentiation, synaptogenesis (Blaesse et al., 2009; Owens and Kriegstein, 2002; Represa and Ben-Ari, 2005) through consequent activation of voltage-gated calcium channels and NMDA receptors (Blaesse et al., 2009; Owens and Kriegstein, 2002). During developmental maturation, the effect of $GABA_A$ receptor activation progressively switches from excitation to inhibition. As the expression of the potassium/chloride co-transporter 2 (KCC2) increases, the subsequent intracellular chloride concentration decreases, inducing $GABA_A$ hyperpolarizing currents, for review see (Briggs and Galanopoulou, 2011). In humans this switch from depolarizing to hyperpolarizing current is proposed to occur around birth (Briggs and Galanopoulou, 2011; Rakhade and Jensen, 2009) based on the developmental patterns of the relative expression of NKCC1 and KCC2 (Dzhala et al., 2005; Vanhatalo et al., 2005). The default of maturation of the inhibitory GABAergic system leads to network hyperexcitability.

Cellular mechanisms triggered by epileptic activity. Early life epilepsy might emerge as a consequence of the impairment of normal developmental reversal potential shift toward more negative values. In this case, downregulation or abnormal expression of KCC2 transporters would be responsible for an abnormal preservation of depolarizing $GABA_A$ after birth. Indeed sustained hyperexcitability of neuronal epileptic networks leads to excessive glutamate release, extrasynaptic NMDA receptor activation, extrasynaptic calcium entry, calpain activation, and KCC2 cleavage (Lee et al., 2011; Puskarjov et al., 2012; Zhou et al., 2012). According to this mechanism, glutamate-induced downregulation of some KCC2 transporters has a long-term potential (hours-days) to inhibit the capacity of some pyramidal cells to extrude chloride during high interneuronal activity, and would facilitate a dynamic shift (seconds) of E_{GABA} toward more positive values. This shift might occur during any form of prolonged hyperexcitability. A loss of inhibition due to the impairment of interneuronal discharges (caused by *SCN1A*+/- or other mutations leading to E/I unbalance) might lead to constitutive depolarized E_{GABA} in some neurons and susceptibility to evoke a dynamic E_{GABA} shift in other neurons.

Although no experimental data have demonstrated yet that E_{GABA} in DS is depolarizing in a subpopulation of interneurons, our results favor this mechanism to explain the emergence of this infant-onset epilepsy. Note that, except for the modification of the sigmoid representing the firing rate of interneurons, our computational model is not specific of DS and could be used to reproduce several types of early onset epilepsies.

Activity-dependent switch of E_{GABA} before seizure

The "static" view of a constitutive depolarizing GABA (combined with upregulation of glutamatergic conductance) might account for a sustained hyperexcitability, but it did not explain the dynamic transitions from background activity to seizures. However, once expression of chloride transporter is downregulated, the efficiency of chloride extrusion out of the cell decreases. Therefore the increase of

ACCEPTED MANUSCRIPT

interneuronal discharges leads to an increased amount of GABA release, and GABA receptor activation could more easily load the targeted cells, shifting E_{GABA} to more depolarized values. Indeed the high frequency discharge of interneurons evokes a dynamic switch of the $GABA_A$ IPSC from hyperpolarizing to depolarizing (Kaila et al., 1997). Recently, it has been shown that basket cells hyperactivity induced by direct optogenetic activation is able to overload pyramidal cells in chloride through $GABA_AR$. Selective activation (Channel rhodopsin-2-mediated) of somatic-targeting parvalbumin-expressing (PV+) interneurons generated excitatory GABAergic responses in pyramidal neurons, which were sufficient to elicit and entrain synchronous discharges across the network (Ellender et al., 2014). Brief (1–10 s) activation of halorhodopsin expressed in Basket-cells caused a positive shift in the GABAergic reversal potential measured in pyramidal cells (E_{GABA} shifts of up to 25 mV) and changed the E/I ratio sufficiently to induce interictal and ictal epileptic activity (Alfonsa et al., 2015; Shiri et al., 2015).

A recent generic computational model called *Epileptor* found that one state variable acting on a very slow time scale (slower than that of spike and wave events) is necessary to capture the time course of the alternating sequence of seizure-like event (SLE) (Jirsa et al., 2014). This slow state variable was shown to guide the entire system, not only between SLEs, but also throughout the SLE time course, and also produced a slow drift of the offset (Jirsa et al., 2014). Indeed, experimental data tends to show that chloride accumulation and extrusion following basket-cell activation is very slow and is in line with the time-varying parameter changes applied in our model to reproduce actual patterns. The time course of the seizure induced by optogenetic overactivation of basket-cells was shown to cause chloride overload and subsequent substantial changes in the GABAergic reversal potential (up to 25 mV) in pyramidal neurons with a slow time constant of 8.0+/- 2.8s (Alfonsa et al., 2015).

Fast onset activity: mutual inhibition drops between GABAergic interneurons

The major perisomatic-targeting interneurons (cholecystokinin or parvalbumin-containing interneurons) in the cerebral cortex and hippocampus form mutually exclusive networks (Karson et al., 2009). Fast inhibition between somatic projecting interneurons is important for physiological fast oscillations in the LFP (for review see (Bartos et al., 2007)).In the present study we show that the progressive change from GABAergic IPSP to GABAergic EPSP within the highly interconnected basket cells (through mutual inhibition) excites some of these cells (I1), produces an increase of their mean firing rate and finally generates fast onset activity on the simulated-LFP. Our simulations suggest that the increase of GABA release and the subsequent chloride accumulation into pyramidal neurons initiates seizure activity. These results suggest that progressive Cl^- accumulation within interneurons and the excitation of the interconnected GABAergic neurons is a key mechanism of activity dependent loss of inhibition.

Our results show that a progressive shift to E_{GABA} in Basket-Basket synapses induces a low voltage preictal fast onset activity in the LFP due to a sustained discharge of interneurons. During this period pyramidal cells remain silent. The increase of interneuronal firing rate induces an increase of GABA release and therefore increases the value of $GABA_A$ reversal potential, leading to a progressive drop of inhibition of I1→P as well as a progressive excitation of both interneurons and pyramidal cells. Finally the drop of inhibitory barrage leads to the transition to seizure initiation and pyramidal discharges. This also suggests that the loss of inhibition in the Basket-Basket loop together with a strong mutual inhibition and the resulting GABA overflow initiate the seizure.

ACCEPTED MANUSCRIPT

Several computational studies suggest that the loss of inhibition within the fast GABA interneurons providing somatic inhibition to pyramidal cells induces epileptic high-frequency EEG waves (Molaee-Ardekani et al., 2010; Wendling et al., 2002).This computational prediction was further confirmed experimentally. In the entorhinal cortex of isolated guinea pig brain preparation, it has been shown that fast activity at seizure onset is mediated by GABAergic inhibitory circuits (Gnatkovsky et al., 2008) and pyramidal cells accumulate chloride at seizure onset (Lillis et al., 2012). Massive discharge of interneurons leads to release and exhaustion of presynaptic GABA which precedes ictal discharge, with a progressive shift of E_{GABA} during normal (-62 mV) to interictal (-60mV) to preictal (-46mV) activities in non-fast-spiking GABAergic interneurons (Zhang et al., 2012). These results were further confirmed by the causal demonstration that optogenetic activation of PV interneurons was able to initiate fast onset seizures mediated by GABA release (Shiri et al., 2015).

Simulated to real EEG: the model reproduces individual EEG patterns observed in Dravet patients

In DS, intracranial EEGs are not available, as patients are not candidate for epilepsy surgery. One limitation of this study is that neural mass models are intended to simulate local neuronal activity, as recorded using intracranial electrodes in animals models or in patients (Wendling et al., 2015). The simulation of scalp EEG signals requires additional extensions related to i) neural field models, ii) brain connectivity and iii) EEG forward problem solution. These extensions are beyond the scope of this study.

A major difference between LFPs and surface recording is related to the attenuation of the signal amplitude. However, when the conductivity of the different layers of the volume conductor is low (typically in infants, as in this study), the temporal dynamics of LFPs generated in the neocortex are conserved in scalp EEG signals collected by nearby electrodes (Lopes da Silva, 2013). These considerations led us to compare both simulated and real signals according to morphological and spectral features, regardless of the amplitude.

There is a high inter-individual diversity of EEG patterns in Dravet patients (Bureau and Bernardina, 2011). Interictal patterns may be either normal or vary from focal, multifocal or generalized spikes occasionally followed by slow waves (Specchio et al., 2012). Some studies also reported an unusual interictal combination of frontal slow bi- or triphasic spikes followed by slow waves when awake and activated by sleep with 5—10 s discharges of 8—9 Hz spikes in a minority of adolescents with DS (Nabbout et al., 2008). Ictal EEG also can show several aspects: a stereotyped pattern of multiple spikes without wave or trains of biphasic/triphasic spikes; a fast rhythm, which is directly diffuse of high voltage, stopping abruptly; a short period of EEG flattening or a fast recruiting rhythm that can be interrupted by flattening, followed by slow waves or irregular diffuse slow wave spikes have also been described (Bureau and Bernardina, 2011). Our results show that this diversity is captured by the model.

Pharmacology in DS

Dravet syndrome is a highly refractory form of epilepsy and intractability of seizures has been included in the criteria of diagnosis by the International League against Epilepsy (1989). Among the conventional antiepileptic drugs, valproate and benzodiazepines are the first line compounds most often used in clinical practice, but their efficacy is uncomplete (Dravet and Oguni, 2013). We also observed a partial

ACCEPTED MANUSCRIPT

effect of BZD on seizures in our computational model. Our results show that, although GABA might still be depolarizing in a sub-population of neonatal neurons, the anticonvulsive effect of BZDs is possibly due to shunting inhibition or inhibition via excitatory effects upon inhibitory interneurons as suggested by (Briggs and Galanopoulou, 2011; Staley, 1992).

Prospective studies suggest that new therapeutics may also be beneficial for children with Dravet syndrome, such as topiramate (Coppola et al., 2002), levetiracetam (Striano et al., 2007), or ketogenic diet (Nabbout et al., 2011), but only stiripentol has demonstrated efficacy using the randomized-controlled methodology (Chiron et al., 2000). Stiripentol is known to increase the duration of $GABA_A$ receptors opening time (Quilichini et al., 2006), preferentially acting on the δ and α3 subunits (Fisher, 2011). To date there is no experience of any monotherapy in Dravet patients. Stiripentol efficacy was demonstrated as adjunctive therapy to valproate and clobazam (Chiron et al., 2000; Inoue et al., 2014; Kassaï et al., 2008). It has been first thought that stiripentol effect only lies on pharmacokinetic drug-drug interactions since it inhibits cytochrome P450 enzymes (CYP3A4 and 2C19) in the liver, thus increasing the plasma concentration of clobazam and nor-clobazam (Chiron et al., 2000). In vitro data has shown that stiripentol and benzodiazepines act independently at $GABA_A$ receptors, thus suggesting that their combination may increase the maximum response beyond that of either drug alone via a pharmacodynamic interaction (Fisher, 2011). Nonetheless the antiepileptic effects of stiripentol are not completely understood and may also interfere with the astrocytic lactate shuttle and/or inhibition of Na^+ and Ca^{2+} influx (for recent review see (Verrotti et al., 2016)).

Our computational results provide additional evidence that in the presence of depolarizing GABA, a super-additive anticonvulsive effect of a moderate dose of BZD was observed in presence of stiripentol, as previously underlined (Brigo, 2013). Since stiripentol prolongs the opening duration of GABA receptor and therefore the kinetics of $GABA_A$ mediated IPSC, this drug might maximize the shunting inhibition, (even if E_{GABA} is depolarized) due to the drop of cell membrane resistance. The model therefore predicts that pharmacological tools that increase the duration of $GABA_A$ receptor opening without increasing the amplitude of chloride current will be more efficient to inhibit seizures of patients with Dravet syndrome.

Acknowledgements

This work was performed as part of the Child-Rare-Euro-Simulation (CRESim) project. CRESim was funded by the ERA-NET PRIOMEDCHILD Joint Call in 2010. Members of the CRESim Project Group: Leon Aarons, Corinne Alberti, Agathe Bajard, Pascal Benquet, Yves Bertrand, Frank Bretz, Daan Caudri, Charlotte Castellan, Sylvie Chabaud, Catherine Chiron, Catherine Cornu, Frank Dufour, Nathalie Eymard, Roland Fisch, Renzo Guerrini, Vincent Jullien, Behrouz Kassai, Polina Kurbatova, Salma Malik, Rima Nabbout, Patrice Nony, Kayode Ogungbenro, David Pérol, Gérard Pons, Anna Rosati, Harm Tiddens, Fabrice Wendling. This work was also supported by a grant from “Investissement d'Avenir - ANR-11-INBS-0011” - NeurATRIS : A Translational Research Infrastructure for Biotherapies in Neurosciences”. We thank Prof David J. Mogul for his assistance on manuscript edition.

ACCEPTED MANUSCRIPT

References

Alfonsa, H., Merricks, E.M., Codadu, N.K., Cunningham, M.O., Deisseroth, K., Racca, C., Trevelyan, A.J., 2015. The Contribution of Raised Intraneuronal Chloride to Epileptic Network Activity. J. Neurosci. 35, 7715–7726. doi:10.1523/JNEUROSCI.4105-14.2015

Bartos, M., Vida, I., Jonas, P., 2007. Synaptic mechanisms of synchronized gamma oscillations in inhibitory interneuron networks. Nat. Rev. Neurosci. 8, 45–56. doi:10.1038/nrn2044

Ben-Ari, Y., Gaiarsa, J.-L., Tyzio, R., Khazipov, R., 2007. GABA: A Pioneer Transmitter That Excites Immature Neurons and Generates Primitive Oscillations. Physiol. Rev. 87, 1215–1284. doi:10.1152/physrev.00017.2006

Ben-Ari, Y., Khalilov, I., Kahle, K.T., Cherubini, E., 2012. The GABA Excitatory/Inhibitory Shift in Brain Maturation and Neurological Disorders. The Neuroscientist 18, 467–486. doi:10.1177/1073858412438697

Blaesse, P., Airaksinen, M.S., Rivera, C., Kaila, K., 2009. Cation-chloride cotransporters and neuronal function. Neuron 61, 820–838. doi:10.1016/j.neuron.2009.03.003

Briggs, S.W., Galanopoulou, A.S., 2011. Altered GABA Signaling in Early Life Epilepsies. Neural Plast. 2011, 1–16. doi:10.1155/2011/527605

Brigo, F., 2013. Pharmacodynamic interaction between stiripentol and benzodiazepines: from molecular to clinical studies. Epilepsy Behav. EB 29, 586. doi:10.1016/j.yebeh.2013.09.016

Bureau, M., Bernardina, B.D., 2011. Electroencephalographic characteristics of Dravet syndrome: EEG Characteristics of Dravet Syndrome. Epilepsia 52, 13–23. doi:10.1111/j.1528-1167.2011.02996.x

Chaudhury, S., Sharma, V., Kumar, V., Nag, T.C., Wadhwa, S., 2016. Activity-dependent synaptic plasticity modulates the critical phase of brain development. Brain Dev. 38, 355–363. doi:10.1016/j.braindev.2015.10.008

Cheah, C.S., Yu, F.H., Westenbroek, R.E., Kalume, F.K., Oakley, J.C., Potter, G.B., Rubenstein, J.L., Catterall, W.A., 2012. Specific deletion of NaV1.1 sodium channels in inhibitory interneurons causes seizures and premature death in a mouse model of Dravet syndrome. Proc. Natl. Acad. Sci. 109, 14646–14651. doi:10.1073/pnas.1211591109

Chiron, C., Marchand, M.C., Tran, A., Rey, E., d'Athis, P., Vincent, J., Dulac, O., Pons, G., 2000. Stiripentol in severe myoclonic epilepsy in infancy: a randomised placebo-controlled syndrome-dedicated trial. STICLO study group. Lancet 356, 1638–1642.

Chopra, R., Isom, L.L., 2014. Untangling the dravet syndrome seizure network: the changing face of a rare genetic epilepsy. Epilepsy Curr. Am. Epilepsy Soc. 14, 86–89. doi:10.5698/1535-7597-14.2.86

Claes, L., Del-Favero, J., Ceulemans, B., Lagae, L., Van Broeckhoven, C., De Jonghe, P., 2001. De novo mutations in the sodium-channel gene SCN1A cause severe myoclonic epilepsy of infancy. Am. J. Hum. Genet. 68, 1327–1332. doi:10.1086/320609

Coppola, G., Capovilla, G., Montagnini, A., Romeo, A., Spanò, M., Tortorella, G., Veggiotti, P., Viri, M., Pascotto, A., 2002. Topiramate as add-on drug in severe myoclonic epilepsy in infancy: an Italian multicenter open trial. Epilepsy Res. 49, 45–48.

Cosandier-Rimélé, D., Bartolomei, F., Merlet, I., Chauvel, P., Wendling, F., 2012. Recording of fast activity at the onset of partial seizures: depth EEG vs. scalp EEG. NeuroImage 59, 3474–3487. doi:10.1016/j.neuroimage.2011.11.045

Debanne, D., Thompson, S.M., Gähwiler, B.H., 2006. A brief period of epileptiform activity strengthens excitatory synapses in the rat hippocampus in vitro. Epilepsia 47, 247–256.

Dravet, C., Oguni, H., 2013. Dravet syndrome (severe myoclonic epilepsy in infancy). Handb. Clin. Neurol. 111, 627–633. doi:10.1016/B978-0-444-52891-9.00065-8

Dzhala, V.I., Talos, D.M., Sdrulla, D.A., Brumback, A.C., Mathews, G.C., Benke, T.A., Delpire, E., Jensen, F.E., Staley, K.J., 2005. NKCC1 transporter facilitates seizures in the developing brain. Nat. Med. 11, 1205–1213. doi:10.1038/nm1301

ACCEPTED MANUSCRIPT

Ellender, T.J., Raimondo, J.V., Irkle, A., Lamsa, K.P., Akerman, C.J., 2014. Excitatory Effects of Parvalbumin-Expressing Interneurons Maintain Hippocampal Epileptiform Activity via Synchronous Afterdischarges. J. Neurosci. 34, 15208–15222. doi:10.1523/JNEUROSCI.1747-14.2014

Escayg, A., MacDonald, B.T., Meisler, M.H., Baulac, S., Huberfeld, G., An-Gourfinkel, I., Brice, A., LeGuern, E., Moulard, B., Chaigne, D., Buresi, C., Malafosse, A., 2000. Mutations of SCN1A, encoding a neuronal sodium channel, in two families with GEFS+2. Nat. Genet. 24, 343–345. doi:10.1038/74159

Fisher, J.L., 2011. Interactions between modulators of the GABAA receptor: Stiripentol and benzodiazepines. Eur. J. Pharmacol. 654, 160–165. doi:10.1016/j.ejphar.2010.12.037

Fritschy, J.-M., 2008. E/I balance and GABAA receptor plasticity. Front. Mol. Neurosci. 1. doi:10.3389/neuro.02.005.2008

Glickfeld, L.L., Roberts, J.D., Somogyi, P., Scanziani, M., 2009. Interneurons hyperpolarize pyramidal cells along their entire somatodendritic axis. Nat. Neurosci. 12, 21–23. doi:10.1038/nn.2230

Gnatkovsky, V., Librizzi, L., Trombin, F., de Curtis, M., 2008. Fast activity at seizure onset is mediated by inhibitory circuits in the entorhinal cortex in vitro. Ann. Neurol. 64, 674–686. doi:10.1002/ana.21519

Goodfellow, M., Schindler, K., Baier, G., 2011. Intermittent spike-wave dynamics in a heterogeneous, spatially extended neural mass model. NeuroImage 55, 920–932. doi:10.1016/j.neuroimage.2010.12.074

Hájos, N., Nusser, Z., Rancz, E.A., Freund, T.F., Mody, I., 2000. Cell type- and synapse-specific variability in synaptic GABAA receptor occupancy. Eur. J. Neurosci. 12, 810–818.

Han, S., Tai, C., Westenbroek, R.E., Yu, F.H., Cheah, C.S., Potter, G.B., Rubenstein, J.L., Scheuer, T., de la Iglesia, H.O., Catterall, W.A., 2012. Autistic-like behaviour in Scn1a+/− mice and rescue by enhanced GABA-mediated neurotransmission. Nature 489, 385–390. doi:10.1038/nature11356

Harkin, L.A., McMahon, J.M., Iona, X., Dibbens, L., Pelekanos, J.T., Zuberi, S.M., Sadleir, L.G., Andermann, E., Gill, D., Farrell, K., Connolly, M., Stanley, T., Harbord, M., Andermann, F., Wang, J., Batish, S.D., Jones, J.G., Seltzer, W.K., Gardner, A., Infantile Epileptic Encephalopathy Referral Consortium, Sutherland, G., Berkovic, S.F., Mulley, J.C., Scheffer, I.E., 2007. The spectrum of SCN1A-related infantile epileptic encephalopathies. Brain J. Neurol. 130, 843–852. doi:10.1093/brain/awm002

Holmes, G.L., Khazipov, R., Ben-Ari, Y., 2002. New concepts in neonatal seizures. Neuroreport 13, A3–8.

Huberfeld, G., Wittner, L., Clemenceau, S., Baulac, M., Kaila, K., Miles, R., Rivera, C., 2007. Perturbed Chloride Homeostasis and GABAergic Signaling in Human Temporal Lobe Epilepsy. J. Neurosci. 27, 9866–9873. doi:10.1523/JNEUROSCI.2761-07.2007

Huneau, C., Benquet, P., Dieuset, G., Biraben, A., Martin, B., Wendling, F., 2013. Shape features of epileptic spikes are a marker of epileptogenesis in mice. Epilepsia 54, 2219–2227. doi:10.1111/epi.12406

Inoue, Y., Ohtsuka, Y., STP-1 Study Group, 2014. Effectiveness of add-on stiripentol to clobazam and valproate in Japanese patients with Dravet syndrome: additional supportive evidence. Epilepsy Res. 108, 725–731. doi:10.1016/j.eplepsyres.2014.02.008

Jedlicka, P., Deller, T., Gutkin, B.S., Backus, K.H., 2011. Activity-dependent intracellular chloride accumulation and diffusion controls GABA(A) receptor-mediated synaptic transmission. Hippocampus 21, 885–898. doi:10.1002/hipo.20804

Jiao, J., Yang, Y., Shi, Y., Chen, J., Gao, R., Fan, Y., Yao, H., Liao, W., Sun, X.-F., Gao, S., 2013. Modeling Dravet syndrome using induced pluripotent stem cells (iPSCs) and directly converted neurons. Hum. Mol. Genet. 22, 4241–4252. doi:10.1093/hmg/ddt275

Jirsa, V.K., Stacey, W.C., Quilichini, P.P., Ivanov, A.I., Bernard, C., 2014. On the nature of seizure dynamics. Brain 137, 2210–2230. doi:10.1093/brain/awu133

Kahle, K.T., Merner, N.D., Friedel, P., Silayeva, L., Liang, B., Khanna, A., Shang, Y., Lachance-Touchette, P., Bourassa, C., Levert, A., Dion, P.A., Walcott, B., Spiegelman, D., Dionne-Laporte, A., Hodgkinson, A., Awadalla, P., Nikbakht, H., Majewski, J., Cossette, P., Deeb, T.Z., Moss, S.J.,

ACCEPTED MANUSCRIPT

Medina, I., Rouleau, G.A., 2014. Genetically encoded impairment of neuronal KCC2 cotransporter function in human idiopathic generalized epilepsy. EMBO Rep. 15, 766–774. doi:10.15252/embr.201438840

Kaila, K., Lamsa, K., Smirnov, S., Taira, T., Voipio, J., 1997. Long-lasting GABA-mediated depolarization evoked by high-frequency stimulation in pyramidal neurons of rat hippocampal slice is attributable to a network-driven, bicarbonate-dependent K+ transient. J. Neurosci. 17, 7662–7672.

Karson, M.A., Tang, A.-H., Milner, T.A., Alger, B.E., 2009. Synaptic cross talk between perisomatic-targeting interneuron classes expressing cholecystokinin and parvalbumin in hippocampus. J. Neurosci. Off. J. Soc. Neurosci. 29, 4140–4154. doi:10.1523/JNEUROSCI.5264-08.2009

Kassaï, B., Chiron, C., Augier, S., Cucherat, M., Rey, E., Gueyffier, F., Guerrini, R., Vincent, J., Dulac, O., Pons, G., 2008. Severe myoclonic epilepsy in infancy: a systematic review and a meta-analysis of individual patient data. Epilepsia 49, 343–348. doi:10.1111/j.1528-1167.2007.01423.x

Lamsa, K., Taira, T., 2003. Use-dependent shift from inhibitory to excitatory GABAA receptor action in SP-O interneurons in the rat hippocampal CA3 area. J. Neurophysiol. 90, 1983–1995. doi:10.1152/jn.00060.2003

Lee, H.H.C., Deeb, T.Z., Walker, J.A., Davies, P.A., Moss, S.J., 2011. NMDA receptor activity downregulates KCC2 resulting in depolarizing GABAA receptor–mediated currents. Nat. Neurosci. 14, 736–743. doi:10.1038/nn.2806

Lillis, K.P., Kramer, M.A., Mertz, J., Staley, K.J., White, J.A., 2012. Pyramidal cells accumulate chloride at seizure onset. Neurobiol. Dis. 47, 358–366. doi:10.1016/j.nbd.2012.05.016

Lin, L.-C., Sibille, E., 2013. Reduced brain somatostatin in mood disorders: a common pathophysiological substrate and drug target? Front. Pharmacol. 4. doi:10.3389/fphar.2013.00110

Liu, Y., Lopez-Santiago, L.F., Yuan, Y., Jones, J.M., Zhang, H., O'Malley, H.A., Patino, G.A., O'Brien, J.E., Rusconi, R., Gupta, A., Thompson, R.C., Natowicz, M.R., Meisler, M.H., Isom, L.L., Parent, J.M., 2013. Dravet syndrome patient-derived neurons suggest a novel epilepsy mechanism. Ann. Neurol. 74, 128–139. doi:10.1002/ana.23897

Lopantsev, V., Both, M., Draguhn, A., 2009. Rapid plasticity at inhibitory and excitatory synapses in the hippocampus induced by ictal epileptiform discharges. Eur. J. Neurosci. 29, 1153–1164. doi:10.1111/j.1460-9568.2009.06663.x

Lopes da Silva, F., 2013. EEG and MEG: relevance to neuroscience. Neuron 80, 1112–1128. doi:10.1016/j.neuron.2013.10.017

Marini, C., Scheffer, I.E., Nabbout, R., Suls, A., De Jonghe, P., Zara, F., Guerrini, R., 2011. The genetics of Dravet syndrome. Epilepsia 52 Suppl 2, 24–29. doi:10.1111/j.1528-1167.2011.02997.x

Molaee-Ardekani, B., Benquet, P., Bartolomei, F., Wendling, F., 2010. Computational modeling of high-frequency oscillations at the onset of neocortical partial seizures: From "altered structure" to "dysfunction." NeuroImage 52, 1109–1122. doi:10.1016/j.neuroimage.2009.12.049

Nabbout, R., Copioli, C., Chipaux, M., Chemaly, N., Desguerre, I., Dulac, O., Chiron, C., 2011. Ketogenic diet also benefits Dravet syndrome patients receiving stiripentol: a prospective pilot study. Epilepsia 52, e54–57. doi:10.1111/j.1528-1167.2011.03107.x

Nabbout, R., Desguerre, I., Sabbagh, S., Depienne, C., Plouin, P., Dulac, O., Chiron, C., 2008. An unexpected EEG course in Dravet syndrome. Epilepsy Res. 81, 90–95. doi:10.1016/j.eplepsyres.2008.04.015

Niedermeyer, E., Lopes da Silva, F.H. (Eds.), 2005. Electroencephalography: basic principles, clinical applications, and related fields, 5th ed. ed. Lippincott Williams & Wilkins, Philadelphia.

Olmos-Serrano, J.L., Paluszkiewicz, S.M., Martin, B.S., Kaufmann, W.E., Corbin, J.G., Huntsman, M.M., 2010. Defective GABAergic Neurotransmission and Pharmacological Rescue of Neuronal Hyperexcitability in the Amygdala in a Mouse Model of Fragile X Syndrome. J. Neurosci. 30, 9929–9938. doi:10.1523/JNEUROSCI.1714-10.2010

Owens, D.F., Kriegstein, A.R., 2002. Is there more to gaba than synaptic inhibition? Nat. Rev. Neurosci. 3, 715–727. doi:10.1038/nrn919

ACCEPTED MANUSCRIPT

Palma, E., Amici, M., Sobrero, F., Spinelli, G., Di Angelantonio, S., Ragozzino, D., Mascia, A., Scoppetta, C., Esposito, V., Miledi, R., Eusebi, F., 2006. Anomalous levels of Cl- transporters in the hippocampal subiculum from temporal lobe epilepsy patients make GABA excitatory. Proc. Natl. Acad. Sci. U. S. A. 103, 8465–8468. doi:10.1073/pnas.0602979103

Pathak, H.R., Weissinger, F., Terunuma, M., Carlson, G.C., Hsu, F.-C., Moss, S.J., Coulter, D.A., 2007. Disrupted Dentate Granule Cell Chloride Regulation Enhances Synaptic Excitability during Development of Temporal Lobe Epilepsy. J. Neurosci. 27, 14012–14022. doi:10.1523/JNEUROSCI.4390-07.2007

Pérez-Cremades, D., Hernández, S., Blasco-Ibáñez, J.M., Crespo, C., Nacher, J., Varea, E., 2010. Alteration of inhibitory circuits in the somatosensory cortex of Ts65Dn mice, a model for Down's syndrome. J. Neural Transm. 117, 445–455. doi:10.1007/s00702-010-0376-9

Puskarjov, M., Ahmad, F., Kaila, K., Blaesse, P., 2012. Activity-dependent cleavage of the K-Cl cotransporter KCC2 mediated by calcium-activated protease calpain. J. Neurosci. Off. J. Soc. Neurosci. 32, 11356–11364. doi:10.1523/JNEUROSCI.6265-11.2012

Puskarjov, M., Seja, P., Heron, S.E., Williams, T.C., Ahmad, F., Iona, X., Oliver, K.L., Grinton, B.E., Vutskits, L., Scheffer, I.E., Petrou, S., Blaesse, P., Dibbens, L.M., Berkovic, S.F., Kaila, K., 2014. A variant of KCC2 from patients with febrile seizures impairs neuronal Cl- extrusion and dendritic spine formation. EMBO Rep. 15, 723–729. doi:10.1002/embr.201438749

Quilichini, P.P., Chiron, C., Ben-Ari, Y., Gozlan, H., 2006. Stiripentol, a Putative Antiepileptic Drug, Enhances the Duration of Opening of GABAA-Receptor Channels. Epilepsia 47, 704–716.

Quilichini, P.P., Diabira, D., Chiron, C., Milh, M., Ben-Ari, Y., Gozlan, H., 2003. Effects of antiepileptic drugs on refractory seizures in the intact immature corticohippocampal formation in vitro. Epilepsia 44, 1365–1374.

Rakhade, S.N., Jensen, F.E., 2009. Epileptogenesis in the immature brain: emerging mechanisms. Nat. Rev. Neurol. 5, 380–391. doi:10.1038/nrneurol.2009.80

Represa, A., Ben-Ari, Y., 2005. Trophic actions of GABA on neuronal development. Trends Neurosci. 28, 278–283. doi:10.1016/j.tins.2005.03.010

Rogers, C.J., Twyman, R.E., Macdonald, R.L., 1994. Benzodiazepine and beta-carboline regulation of single GABAA receptor channels of mouse spinal neurones in culture. J. Physiol. 475, 69–82.

Scheffer, I.E., 2012. Diagnosis and long-term course of Dravet syndrome. Eur. J. Paediatr. Neurol. 16, S5–S8. doi:10.1016/j.ejpn.2012.04.007

Scheffer, I.E., Berkovic, S.F., 1997. Generalized epilepsy with febrile seizures plus. A genetic disorder with heterogeneous clinical phenotypes. Brain J. Neurol. 120 (Pt 3), 479–490.

Schiff, S.J., Colella, D., Jacyna, G.M., Hughes, E., Creekmore, J.W., Marshall, A., Bozek-Kuzmicki, M., Benke, G., Gaillard, W.D., Conry, J., Weinstein, S.R., 2000. Brain chirps: spectrographic signatures of epileptic seizures. Clin. Neurophysiol. 111, 953–958. doi:10.1016/S1388-2457(00)00259-5

Shiri, Z., Manseau, F., Lévesque, M., Williams, S., Avoli, M., 2015. Interneuron activity leads to initiation of low-voltage fast-onset seizures. Ann. Neurol. 77, 541–546. doi:10.1002/ana.24342

Specchio, N., Balestri, M., Trivisano, M., Japaridze, N., Striano, P., Carotenuto, A., Cappelletti, S., Specchio, L.M., Fusco, L., Vigevano, F., 2012. Electroencephalographic Features in Dravet Syndrome: Five-Year Follow-Up Study in 22 Patients. J. Child Neurol. 27, 439–444. doi:10.1177/0883073811419262

Staley, K., 1992. Enhancement of the excitatory actions of GABA by barbiturates and benzodiazepines. Neurosci. Lett. 146, 105–107.

Stödberg, T., McTague, A., Ruiz, A.J., Hirata, H., Zhen, J., Long, P., Farabella, I., Meyer, E., Kawahara, A., Vassallo, G., Stivaros, S.M., Bjursell, M.K., Stranneheim, H., Tigerschiöld, S., Persson, B., Bangash, I., Das, K., Hughes, D., Lesko, N., Lundeberg, J., Scott, R.C., Poduri, A., Scheffer, I.E., Smith, H., Gissen, P., Schorge, S., Reith, M.E.A., Topf, M., Kullmann, D.M., Harvey, R.J., Wedell, A., Kurian, M.A., 2015. Mutations in SLC12A5 in epilepsy of infancy with migrating focal seizures. Nat. Commun. 6, 8038. doi:10.1038/ncomms9038

ACCEPTED MANUSCRIPT

Striano, P., Coppola, A., Pezzella, M., Ciampa, C., Specchio, N., Ragona, F., Mancardi, M.M., Gennaro, E., Beccaria, F., Capovilla, G., Rasmini, P., Besana, D., Coppola, G.G., Elia, M., Granata, T., Vecchi, M., Vigevano, F., Viri, M., Gaggero, R., Striano, S., Zara, F., 2007. An open-label trial of levetiracetam in severe myoclonic epilepsy of infancy. Neurology 69, 250–254. doi:10.1212/01.wnl.0000265222.24102.db

Tai, C., Abe, Y., Westenbroek, R.E., Scheuer, T., Catterall, W.A., 2014. Impaired excitability of somatostatin-and parvalbumin-expressing cortical interneurons in a mouse model of Dravet syndrome. Proc. Natl. Acad. Sci. 111, E3139–E3148.

Vanhatalo, S., Palva, J.M., Andersson, S., Rivera, C., Voipio, J., Kaila, K., 2005. Slow endogenous activity transients and developmental expression of K+-Cl- cotransporter 2 in the immature human cortex. Eur. J. Neurosci. 22, 2799–2804. doi:10.1111/j.1460-9568.2005.04459.x

Verrotti, A., Prezioso, G., Stagi, S., Paolino, M.C., Parisi, P., 2016. Pharmacological considerations in the use of stiripentol for the treatment of epilepsy. Expert Opin. Drug Metab. Toxicol. 12, 345–352. doi:10.1517/17425255.2016.1145657

Wendling, F., Bartolomei, F., Bellanger, J.J., Chauvel, P., 2002. Epileptic fast activity can be explained by a model of impaired GABAergic dendritic inhibition. Eur. J. Neurosci. 15, 1499–1508. doi:10.1046/j.1460-9568.2002.01985.x

Wendling, F., Bartolomei, F., Mina, F., Huneau, C., Benquet, P., 2012. Interictal spikes, fast ripples and seizures in partial epilepsies - combining multi-level computational models with experimental data: Computational and experimental models of epilepsy. Eur. J. Neurosci. 36, 2164–2177. doi:10.1111/j.1460-9568.2012.08039.x

Wendling, F., Benquet, P., Bartolomei, F., Jirsa, V., 2015. Computational models of epileptiform activity. J. Neurosci. Methods. doi:10.1016/j.jneumeth.2015.03.027

Xue, M., Atallah, B.V., Scanziani, M., 2014. Equalizing excitation–inhibition ratios across visual cortical neurons. Nature. doi:10.1038/nature13321

Yu, F.H., Mantegazza, M., Westenbroek, R.E., Robbins, C.A., Kalume, F., Burton, K.A., Spain, W.J., McKnight, G.S., Scheuer, T., Catterall, W.A., 2006. Reduced sodium current in GABAergic interneurons in a mouse model of severe myoclonic epilepsy in infancy. Nat. Neurosci. 9, 1142–1149. doi:10.1038/nn1754

Zeilhofer, H.U., Wildner, H., Yevenes, G.E., 2012. Fast Synaptic Inhibition in Spinal Sensory Processing and Pain Control. Physiol. Rev. 92, 193–235. doi:10.1152/physrev.00043.2010

Zhang, Z.J., Koifman, J., Shin, D.S., Ye, H., Florez, C.M., Zhang, L., Valiante, T.A., Carlen, P.L., 2012. Transition to Seizure: Ictal Discharge Is Preceded by Exhausted Presynaptic GABA Release in the Hippocampal CA3 Region. J. Neurosci. 32, 2499–2512. doi:10.1523/JNEUROSCI.4247-11.2012

Zhou, H.-Y., Chen, S.-R., Byun, H.-S., Chen, H., Li, L., Han, H.-D., Lopez-Berestein, G., Sood, A.K., Pan, H.-L., 2012. N-methyl-D-aspartate receptor- and calpain-mediated proteolytic cleavage of K+-Cl- cotransporter-2 impairs spinal chloride homeostasis in neuropathic pain. J. Biol. Chem. 287, 33853–33864. doi:10.1074/jbc.M112.395830

ACCEPTED MANUSCRIPT

Figures Legends

Fig 1. Computational Neural mass model of epileptic activity.

(**A**) Structure of the neuronal population model accounting for three sub-populations of neurons: (i) pyramidal cells (P), (ii) soma- and proximal-dendrite-targeting cells (type I1 mediating $GABA_A$, fast currents), and (iii) dendrite-targeting cells (type I2 mediating $GABA_A$, slow). Pyramidal cells receive excitatory input from other pyramidal cells (collateral excitation) or inhibitory input from interneurons. These latter cells receive excitatory input only from pyramidal cells. Besides synaptic transmission, interactions between neuronal subpopulations are also characterized in the model by connectivity constants (CPP, CPI_1, CI_1P, CI_1I_1, CPI_2, CI_2P) which account for the average number of active synaptic contacts or "connection strength" between considered sub-populations. In addition, the nonspecific influence from neighboring or distant populations is represented by a Gaussian input noise *p(t)* corresponding to an excitatory input that globally describes the average density of afferent action potentials (Adapted from Molaee-Ardekani et al, 2010).

(B) The classical wave-to-pulse function was modified to account for the SCN1A mutation found in the Dravet syndrome. According to the neural mass modeling approach, the wave-to-pulse function relates the average pulse density of action potentials fired by the neurons $S_{\mathrm{x}}(\vartheta)$ to the average postsynaptic potential ϑ (in mV) and accounts for the saturation and threshold effects taking place at the soma. For a given sub-population X, it is modeled by a static nonlinear function of sigmoidal shape $S_{\mathrm{x}}(\vartheta) = Q_{\mathrm{x}}^{\max}/(1 + e^{\mathrm{r_x}(\vartheta_{\mathrm{x}} - \vartheta)})$ where $Q_{\mathrm{x}}^{\max}$ is the maximum firing rate, $\mathrm{r_x}$ is the steepness of the sigmoid and ϑ_{x} is the postsynaptic potential corresponding to a firing rate of $Q_{\mathrm{x}}^{\max}/2$. In the proposed DS model (green line), $Q_{\mathrm{x}}^{\max}$ parameter for both inhibitory sub-populations (I1 and I2) was reduced by 40% as compared with the pyramidal cell sub-population (black solid line). This reduction accounts for a strong decrease of the maximal interneuronal firing rate found in DS.

(**C**) Static depolarizing GABA. Left: In normal tissue, the high expression of chloride transporters in the GABAergic post-synaptic compartment, allows efficient extrusion of chloride outside the targeted neuron, responsible for hyperpolarized reversal potential (E_{Cl}=-80mV) of $GABA_A$ IPSP. Right: In epileptic tissue, the expression of chloride transporter at the membrane is decreased at least in some neurons, leading to a "static" more positive reversal potential (E_{Cl}=-60mV) of $GABA_A$ IPSP.

(D) Time course of the average excitatory and inhibitory postsynaptic potentials (PSPs) in the DS model. Depolarizing GABA was implemented in the model as an excitatory signal obeying the kinetics of $GABA_A$-mediated PSP (red line).These kinetics are defined by the time constant used the pulse-to-wave function (either excitatory or inhibitory) that determines both the rise time (t_{rise}) and the decay time (t_{decay}) of the PSP. As t_{rise} and t_{decay} depend mainly on intrinsic ionotropic channel properties and as the direction of the current depends mainly on the reversal potential of chloride, we modified the direction of the depolarizing $GABA_A$ related PSP but not its kinetics.

(**E**) Dynamic depolarizing GABA. Left: In the epileptic tissue a slightly decreased expression of the chloride transporter, could lead to normal IPSP (E_{Cl} =-80mV) when the interneuronal activity is low. Right: When interneurons fire with a high frequency rate, it leads to massive GABA release and chloride overload into the targeted cell, and progressively and dynamically shifts E_{Cl} toward depolarized potential. Therefore if interneurons firing rate dramatically increases it induces a dynamic shift of $GABA_A$-mediated post synaptic potentials from inhibitory to excitatory effect.

ACCEPTED MANUSCRIPT

Fig 2. Depolarizing $GABA_A$ generates spontaneous transitions from interictal to seizure-like activity.

A: Simulated EEG activity during the progressive increase of the fraction of excitatory vs. inhibitory PSPs mediated at $GABA_A$ receptors (depolarizing GABA effect). The tuning of this single parameter is sufficient to elicit a transition from interictal to ictal activity. Dynamic changes from background activity to seizure termination are observed as reflected by simulated signals sequentially exhibiting epileptic spikes, chirp-like fast onset (FO) activity and seizure-like activity.

(**B**) Magnification of the fast onset activity simulated in Fig 1A. Time-frequency analysis (spectrogram) of the signal shows that the fast onset activity starts around 100 Hz. Both the frequency and energy progressively decrease with time. These signal features are reminiscent of the chirp-like activity often encountered at the onset of seizures.

(C) Average firing rate of neuronal sub-populations (Blue: pyramidal cells - P –, Red: somatic-projecting interneurons - I1 – and Green: dendritic-projecting interneurons - I2 -) during the local field activity presented in A. An increase of the firing rate of P, I1 and I2 during interictal epileptic spikes and ictal-like activity is observed. In contrast, before and during seizure onset, the increase of the firing rate is limited to I1 and I2. The inset shows the high frequency of I1 subpopulation during the chirp-like activity at seizure onset. The thin gray line indicates the correspondence of the firing rate of the three subpopulations of neurons with the mean field activity depicted in Fig 1A.

(D) Simulated EEG activity, with the same parameters as in A, but left panel: without depolarizing $GABA_A$ from dendritic-projecting interneurons to pyramidal cells (I2→P) middle panel: without depolarizing $GABA_A$ from somatic-projecting interneurons to themselves (I1→I1), right panel: without depolarizing $GABA_A$ from somatic-projecting interneurons to pyramidal cells (I1→P). Note that depolarizing $GABA_A$ from I1→I1 and I1→P are required to trigger seizure-like activity.

Fig 3. Comparison of simulated and real interictal epileptic spikes from Dravet syndrome patients

(**A**) Example of simulated EEG activity showing that "Dynamic depolarizing $GABA_A$" (I1->P and from I1->I1) is sufficient to produce different morphologies of interictal spikes.

(**B**) The different types of interictal spikes produced by the model and comparison with real EEG signals recorded in DS children. The gray rectangles on each neuronal population model scheme indicate the parameters of the model that were changed comparing to 'parameters of base' (Table 1).

(**C**) Results suggest that "dynamic depolarizing $GABA_A$" from I1->P induces progressive increase of the amplitude of the wave following epileptic interictal spikes. Scale bar: 200 μV.

Fig 4. Comparison of simulated and real ictal epileptic patterns from Dravet syndrome patients.

Different types of real ictal activity recorded in DS children (left column) and comparison with ictal activity produced by the model (middle column). Right column shows neuronal population model schemes with gray rectangles, indicating the parameters of the model that were changed comparing to 'parameters of base' (Table 1). Scale bar: 200 μV.

ACCEPTED MANUSCRIPT

Fig 5. Dynamic shift of depolarizing $GABA_A$ during seizures evokes features changes of EEG patterns. (**A**)Example of ictal activity recorded in DS patient, showing the progressive change of EEG morphology in course of the seizure (different patterns are indicated by circles, asterisks and criss-crosses). The pattern illustrated here was recorded in frontal cortex of patient 3, 10 seconds after seizure initiation. (**B**) Comparison of simulated EEG signals (right column) to real ictal EEG morphologies (left column) from (A). (**C**) Simulated ictal activity, suggesting that different seizure morphologies observed in course of seizure are evoked by that "dynamic depolarizing $GABA_A$" from I1->I1. In the simulation $dGABA_A$ in the inhibitory loop was very high during the first period of the seizure and then progressively returned to normal values. Scale bar: 200 μV.

Fig 6. Simulated effect of Stiripentol and benzodiazepine on ictal-like activity. (**A**) Example of simulated course of seizure with background activity with interictal spikes at the beginning following by fast-onset activity, seizure and seizure termination. (**B**) Action of Stiripentol (STP) on the course of seizure (A) is presented. STP enhances the activity of the $GABA_A$ receptors. Examination of mIPSCs (miniature $GABA_A$ receptor–mediated currents) kinetics indicated that STP also markedly increased the mIPSC decay-time constant [12]. Enhanced activity of the $GABA_A$ receptors increased shunting effect. We represented shunting effect in the model by reducing the membrane potential with increasing of IPSPS decay-time constant. Prolonged IPSC decay time is concentration dependent. (**C**) Action of benzodiazepine (BZD), increasing the amplitude of IPSC, on the course of seizure (A) is presented. (**D**) Combined action of BZD and STP conducts to background activity.

Supporting Information Figure legend

S1 Fig. Robustness of the identified interictal/ictal transition pattern. Up to 40% change of both parameters alpha_I1_P and alpha_I1_I1, the sequence of phases (background activity, sporadic/rhythmic spikes, fast onset activity, ictal activity) is preserved.

ACCEPTED MANUSCRIPT

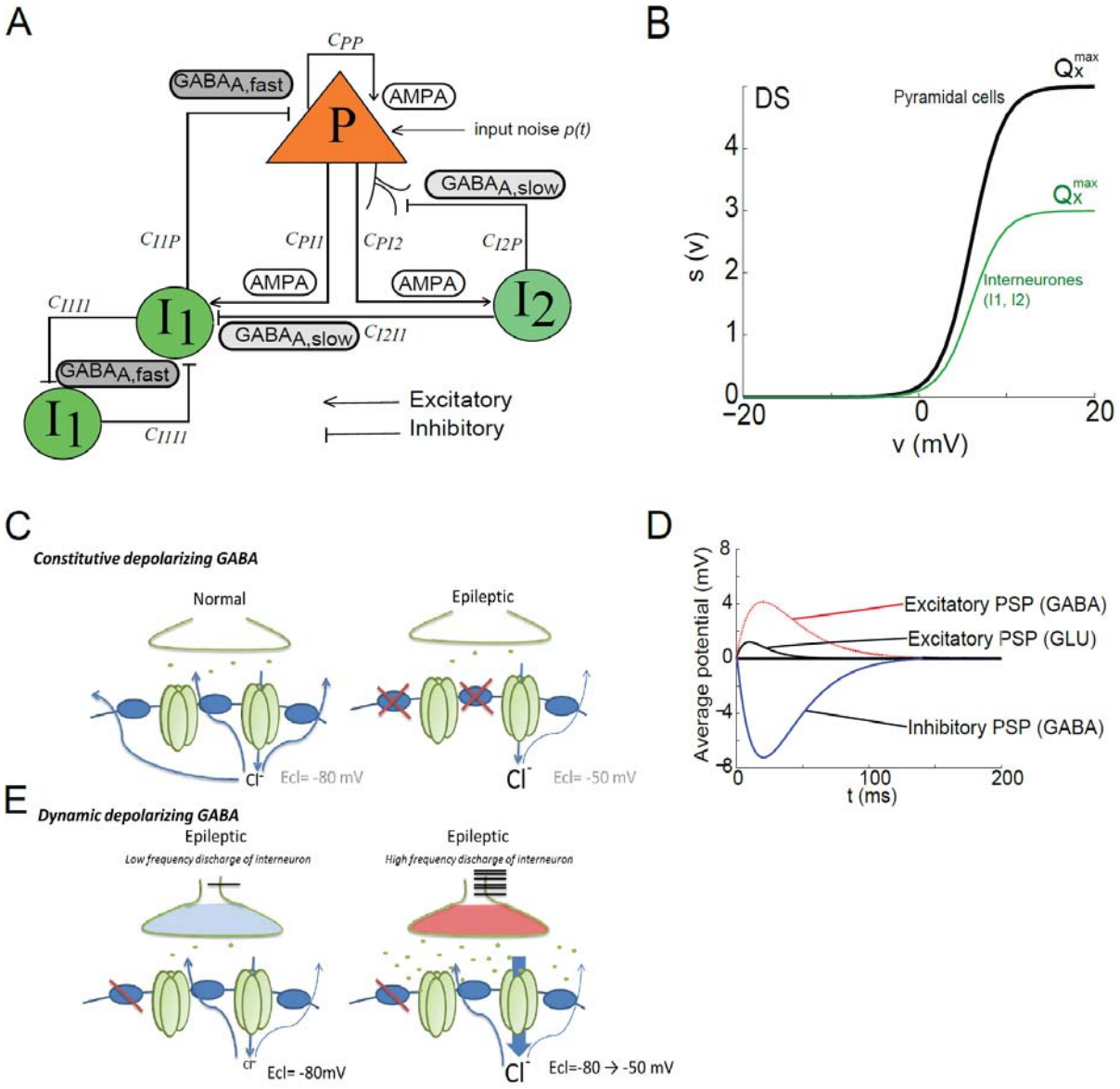

Fig. 1

ACCEPTED MANUSCRIPT

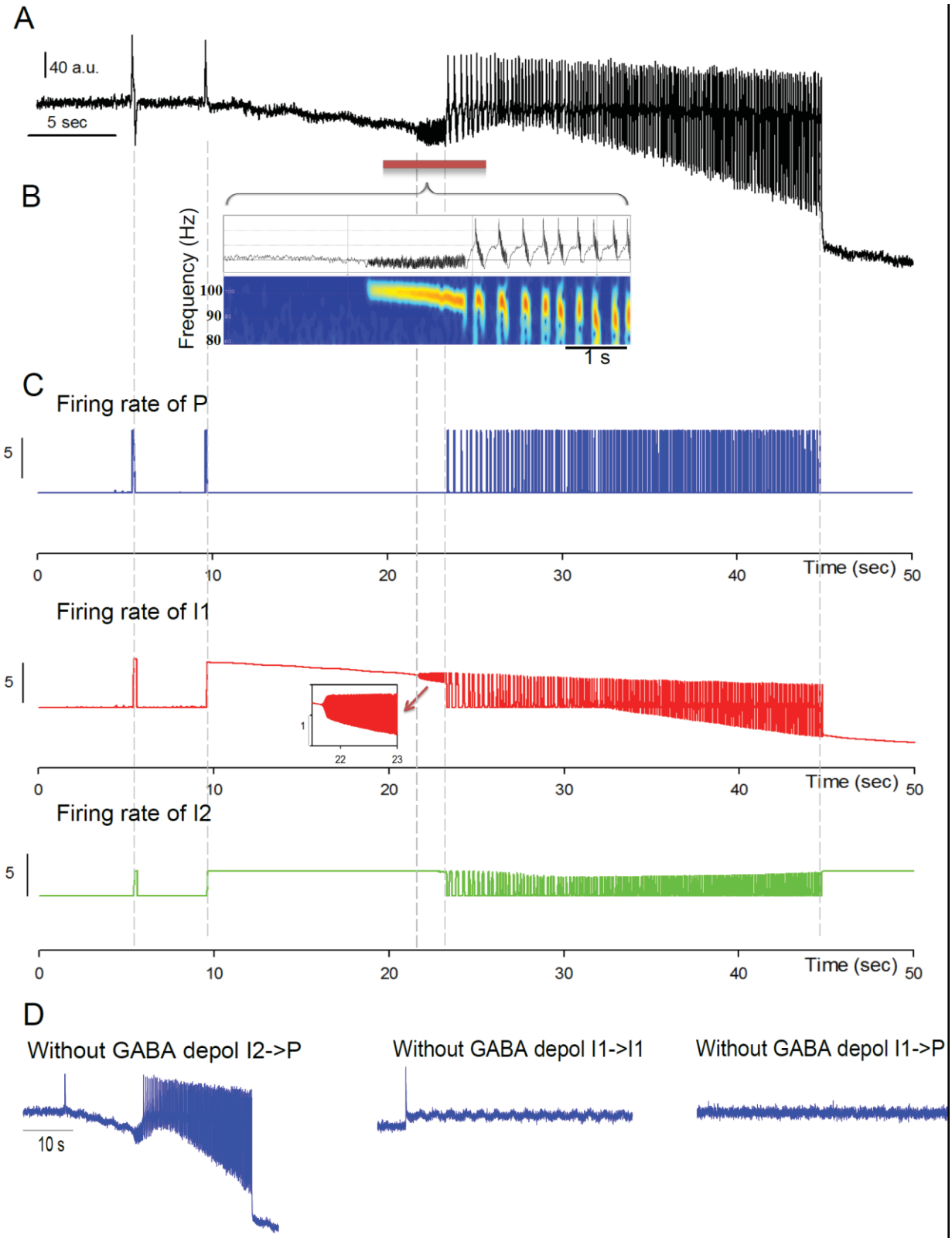

Fig. 2

ACCEPTED MANUSCRIPT

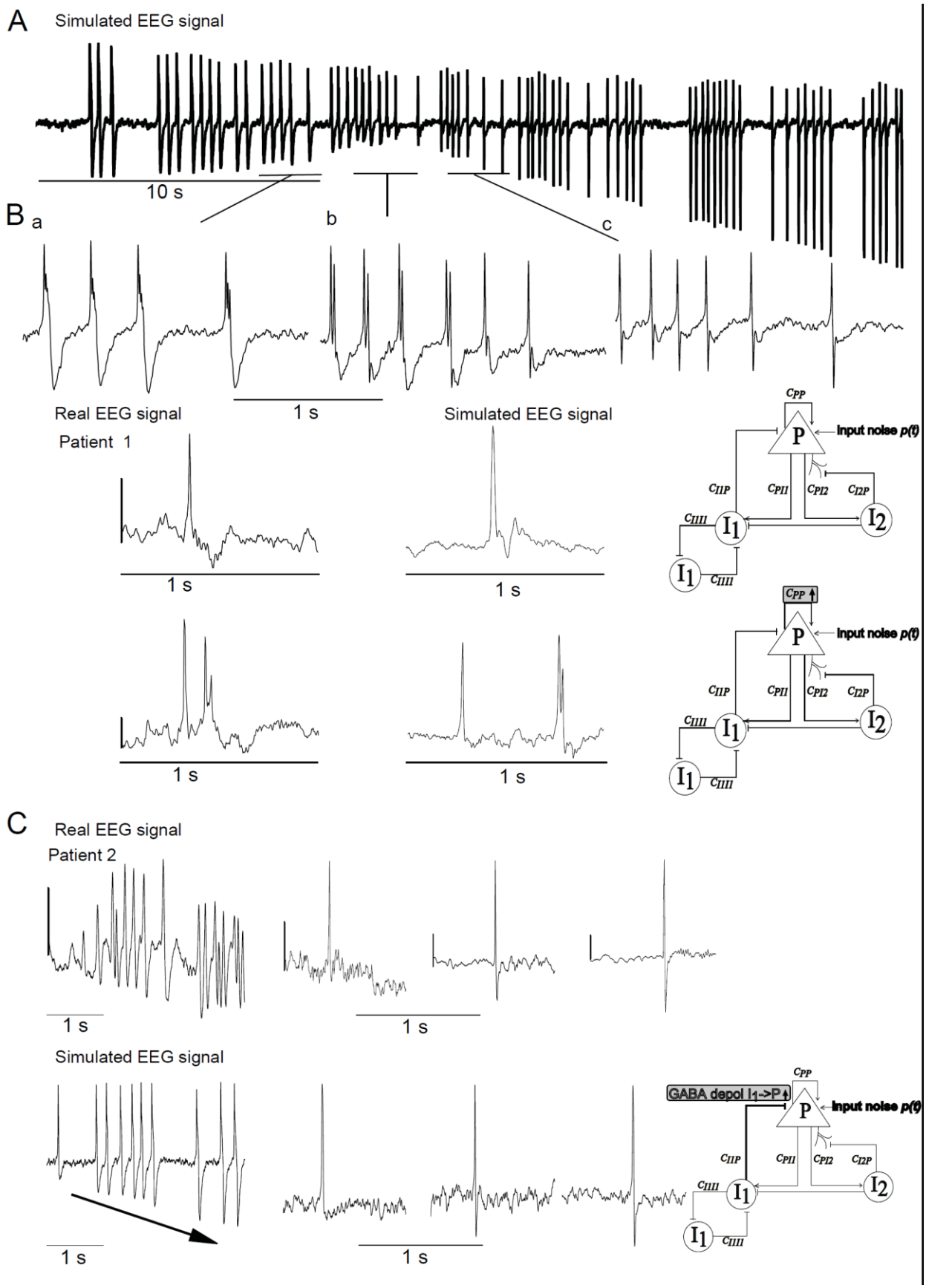

Fig. 3

ACCEPTED MANUSCRIPT

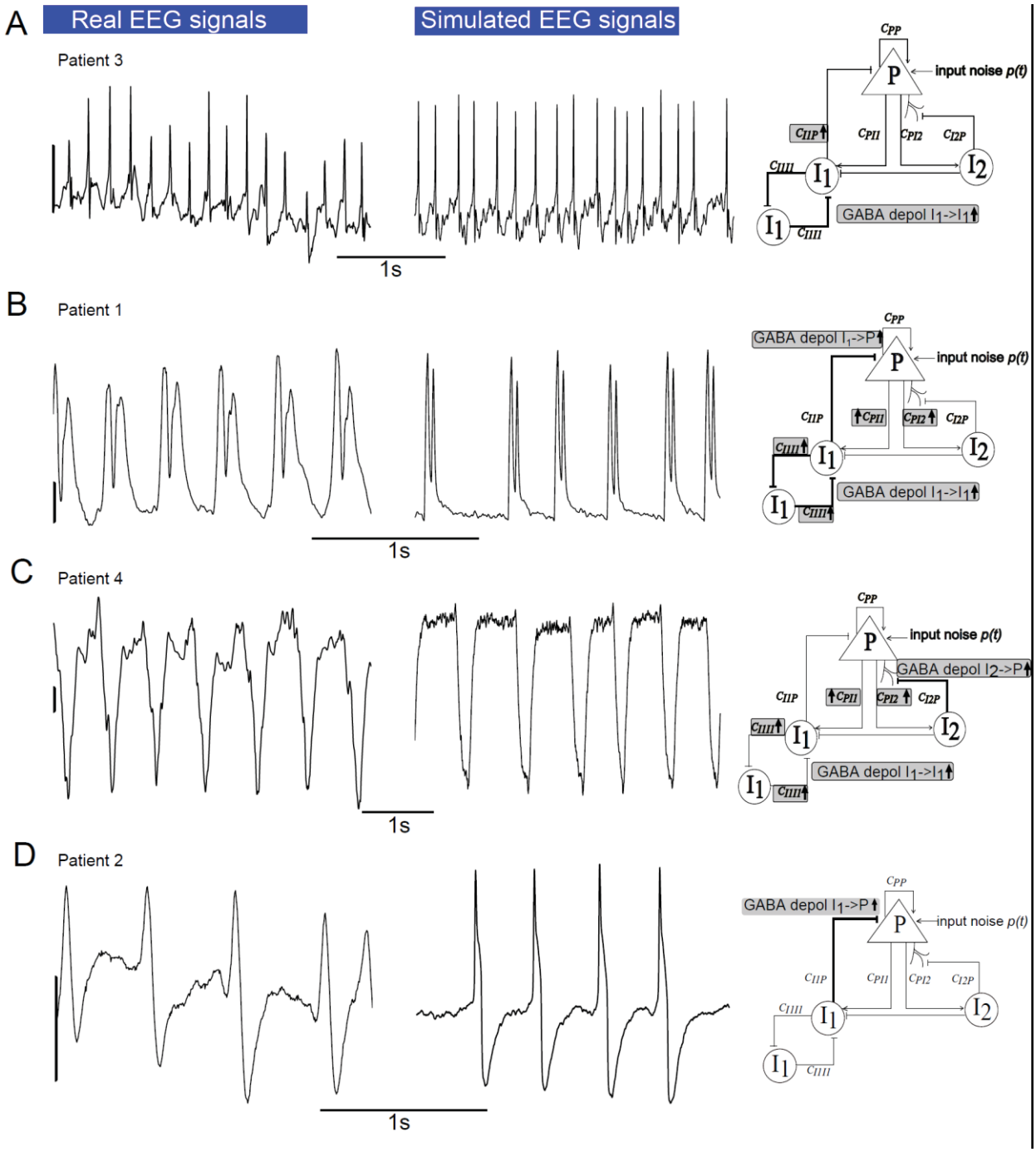

Fig. 4

ACCEPTED MANUSCRIPT

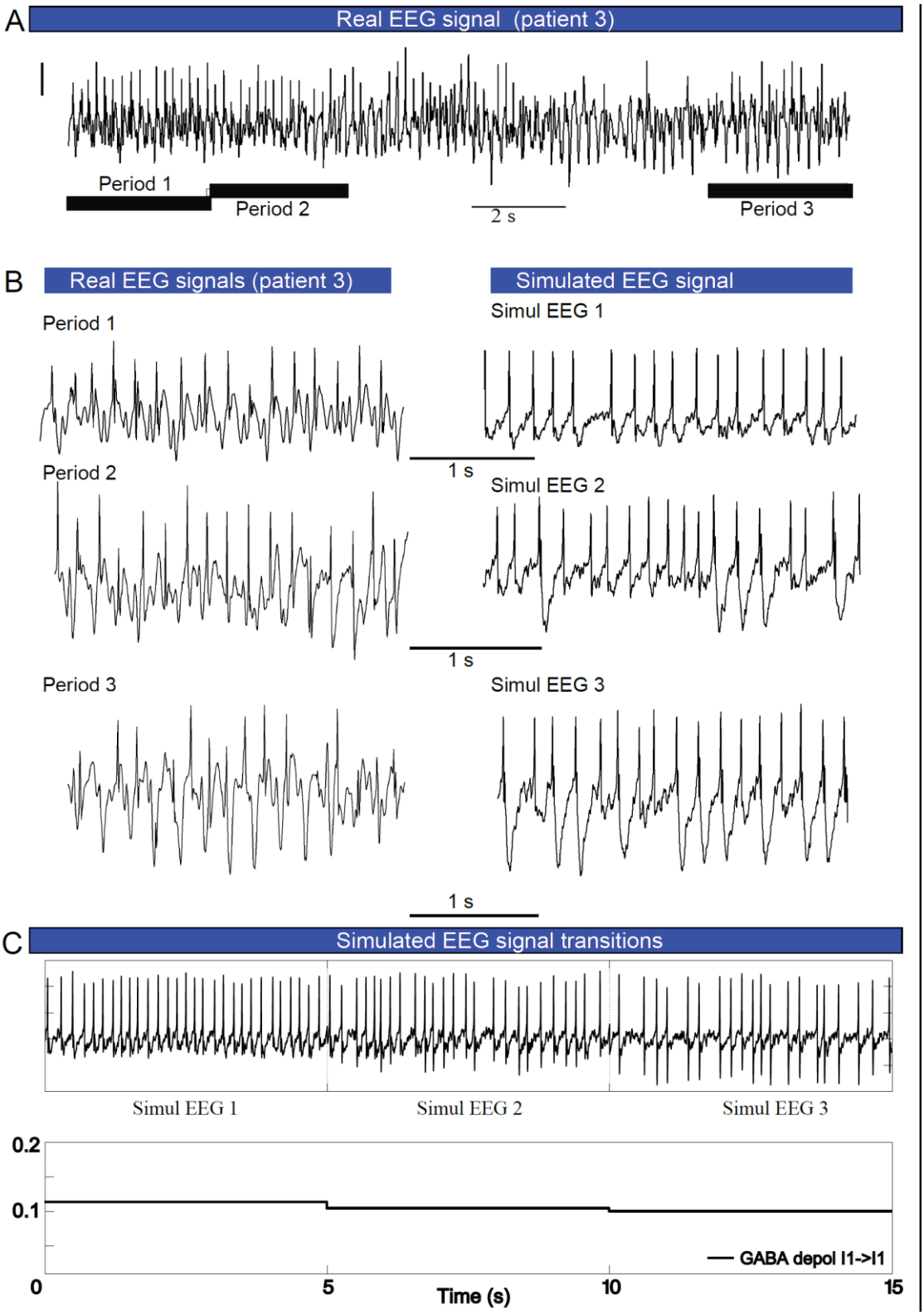

Fig. 5

ACCEPTED MANUSCRIPT

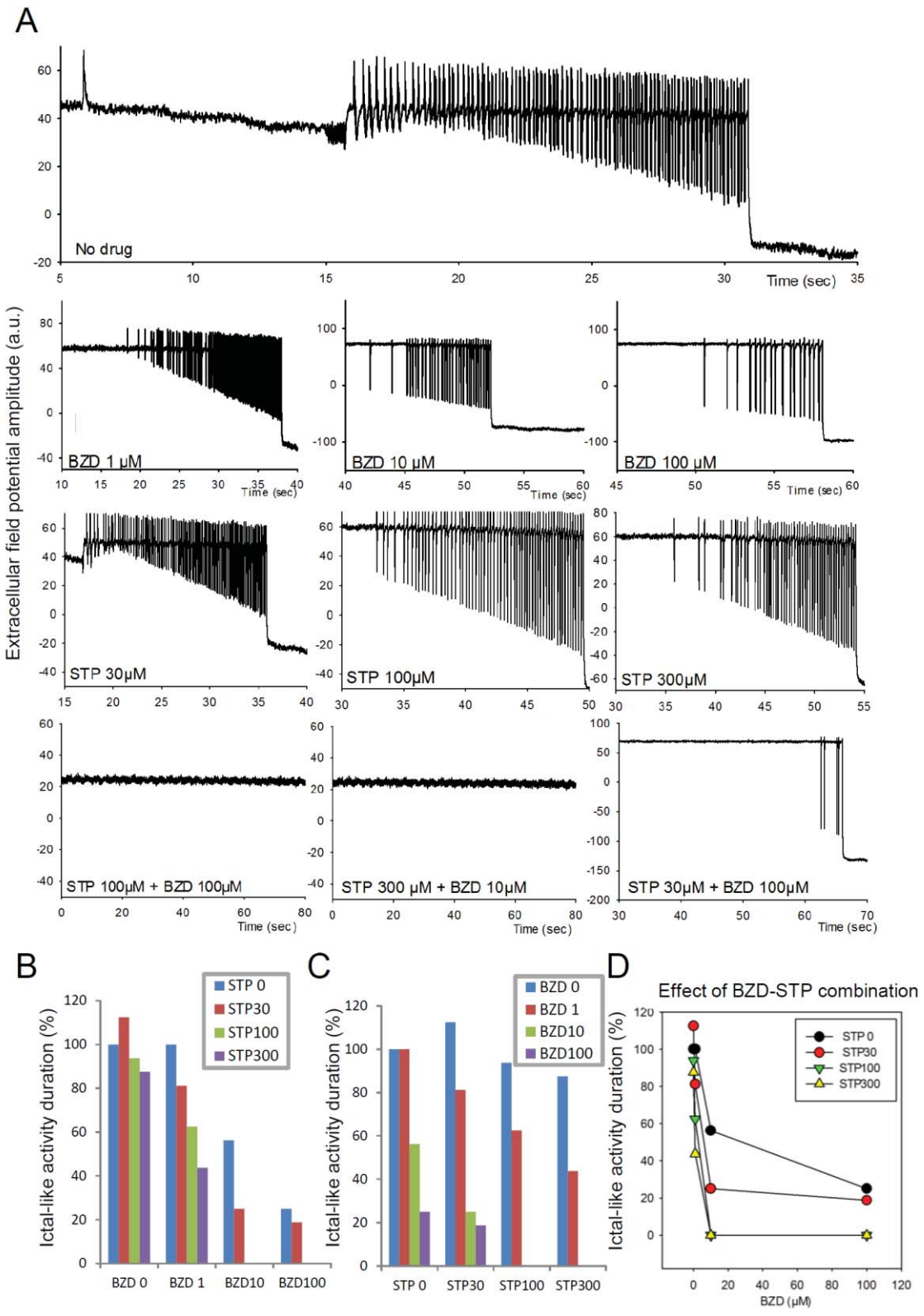

Fig. 6

ACCEPTED MANUSCRIPT

TABLE 1. Model parameters.

Significance		Fig 2	Fig 2 and 6	Fig 3	Fig 3 B	Fig 3C	Fig 4 A	Fig 4 B	Fig 4 C	Fig 4 D	Fig 5
		Fast onset activity	Spont.transition from bckg to seizure like activity	Series of epileptic spikes	Interictal spikes	Evolution of spike shape	Seizure-like activity	Seizure-like activity	Seizure-like activity	Seizure-like activity	Evolution of seizure patterns
Average synaptic contact x→x	C_{PP}	80	80	110	110	110	90	50	65	110	75
	C_{PI1}	20	20	40	20	40	22	400	80	40	22
	C_{I1I1}	15	15	25	15	15	20	60	70	15	21
	C_{I1P}	80	80	55	80	60	118	100	50	60	118
	C_{PI2}	5	5	6	5	6	10	50	15	6	10
	C_{I2P}	20	20	20	20	20	16.5	25	20	20	16.5
Constant or time-dependent parameter in GABA	α_{I1P}	0.017	0.017	0.0015	0.0005	0.085	0.14	0.119	0.019	0.017	0.17
	α_{I1I1}	0.007	0.007	0.0086	0.067	0.017	0.13	0.39	0.075	0.085	0.118
Mean PSP amplitude (AMPA, GABA a, s GABA a,f)	W_{AMPA}; $W_{GABAa,s}$; $W_{GABAa,f}$	5; 50; 20									
Kinetic of PSP(AMPA, GABA a, s GABA a,f)	$1/\tau_{AMPA}$; $1/\tau_{GABAa,s}$; $1/\tau_{GABAa,f}$	180; 33; 220									
Wave to pulse function in subpopulation x.	Θ_P; Q_P^{max} ; r_P	6; 8; 1.2									
	Θ_{I1}; Q_{I1}^{max}; r_{I1}	8; 4.8; 0.5									
	Θ_{I2}; Q_{I2}^{max}; r_{I2}	8; 4.4; 0.5									

ACCEPTED MANUSCRIPT

TABLE 2. Demographic data of patients.

Patient	BA (pt 1)	NP (pt 2)	DD (pt 3)	EM (pt 4)
Age of onset	4 m	4.5 m	7 m	6 m
Age	9 y	14 y	3y 2m	8 y
First seizure				
Type	Clonic unilat. sn	GTC	GTC	Clonic unilat. dx
Duration	30 min	25 min	20 min	20 min
Fever association	Yes	Yes	Yes	Yes
Vaccine association	Yes	No	No	No
Interictal EEG	nl	nl	nl	nl
PMD	nl	nl	nl	nl
AED (after 1st seizure)	CBZ	VPA	VPA	VPA
Other reported seizures'types				
Myoclonic attacks	Yes	Yes	Yes	Yes
Myoclonic status	No	No	Yes	Yes
GTCS	Yes	Yes	Yes	Yes
Unilateral motor	Yes	Yes	No	Yes
Atypical absences	Yes	No	No	Yes
Partial seizures	No	Yes	No	Yes
Tonic (age of onset-end)	2 y 10 m - ?	No	y (3-5y)	4 y - ?
Fever sensitivity	+++	+++	++	++
Seizure in cluster	No	Yes	Yes	Yes
Treatment (onset-end)				
VPA	14 m - now	5.5m -	11m -	6 m - now
FB	6 m – 2 y 7 m	No	No	Yes
CLB	4 y - now	5y -	2.5y -	1 y - now
CLZ	14 m – 3 y	No	No	No
NZP	No	No	No	Yes
STP	2 y 7 m – 4 y 8 m	7y -	2.5y -	1 y - now
TPM	No	12-13y	7y -	5 y – 6 y
ETS	2 y 10 m - 4 y 8 m	No	No	No
CBZ	5 m – 6 m	No	No	Yes
VGB	No	No	No	No
PHT	No	No	No	? - 1 y 9 m
LVC	No	13y-	No	? - 7 y
LTG	No	5-5.5y	No	No
PRM	No	No	No	Yes
ZNS	No	No	No	7 y – 7 y 9 m
Hydrocortisone	4 y 8 m - ?	No	No	5 y 8 m – 6 y
Ketogenic diet	No	No	No	Yes
Vagal stimulator	No	No	No	No
Language	Simple S	short sentences	isolated words	No
Psychomotor delay	Moderate	moderate	severe	Moderate- Severe
***SCN1A* mutations**	c.680 T>C	C3880-1G>T intron 19	C4582-1G>T	IVS8+1C>T

ACCEPTED MANUSCRIPT

Highlights

- Excitatory GABA effect was implemented in a computational neural mass model
- Dynamic emergence of depolarizing GABA triggers interictal to ictal transitions
- Results suggest a major role of GABAergic interneurons in seizure onset
- Model reproduces clinical patterns found in a severe infantile epilepsy

ACCEPTED MANUSCRIPT